



**POLITECNICO**  
MILANO 1863

DIPARTIMENTO DI MECCANICA



## Recent advances and directions in the development of bioresorbable metallic cardiovascular stents: Insights from recent human and in vivo studies

Oliver, A. A.; Sikora-Jasinska, M.; Demir, A. G.; Guillory, R. J.

This is a post-peer-review, pre-copyedit version of an article published in Acta biomaterialia. The final authenticated version is available online at:

<http://dx.doi.org/10.1016/j.actbio.2021.03.058>

This content is provided under [CC BY-NC-ND 4.0](https://creativecommons.org/licenses/by-nc-nd/4.0/) license



# Recent advances and directions in the development of bioresorbable metallic cardiovascular stents: Insights from recent human and in vivo studies

Alexander A. Oliver<sup>1\*</sup>, Malgorzata Sikora-Jasinska<sup>2</sup>, Ali Gökhan Demir<sup>3</sup>, Roger J. Guillory II<sup>1\*</sup>

*1: Department of Biomedical Engineering, Michigan Technological University, USA*

*2: Department of Materials Science and Engineering, Michigan Technological University, USA*

*3: Department of Mechanical Engineering, Politecnico di Milano, IT*

\*Co-corresponding authors:

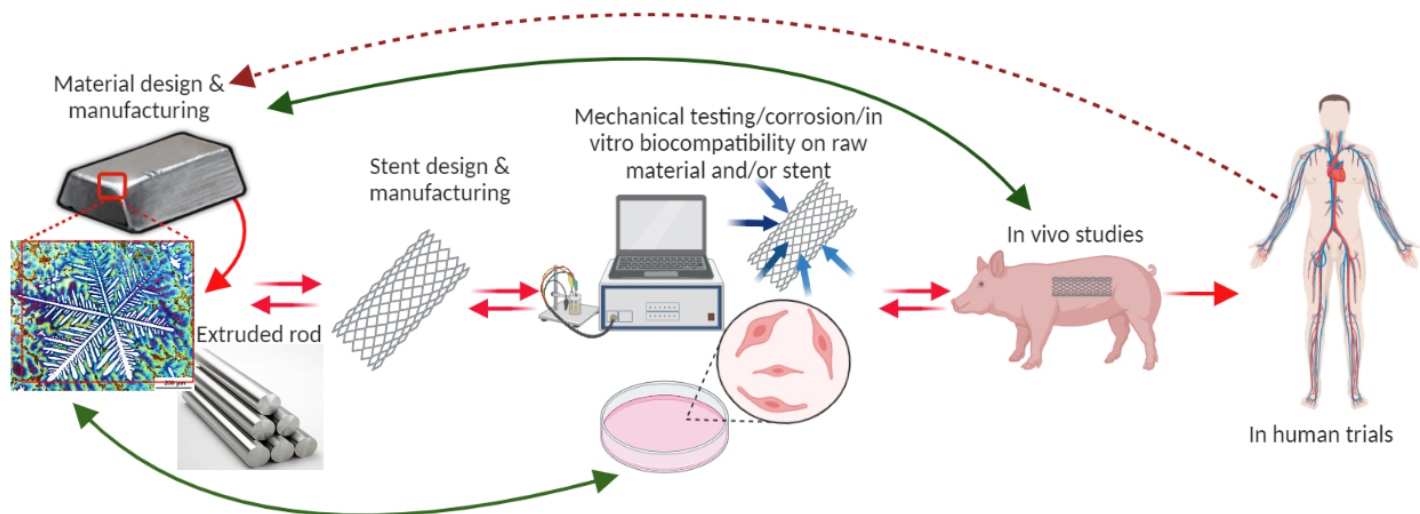
Roger Guillory, Ph.D.,  
Assistant Professor  
Biomedical Engineering Department  
Michigan Technological University  
Houghton, MI, 49931 USA  
Phone: 906-487-3562  
Email: [rjguillo@mtu.edu](mailto:rjguillo@mtu.edu)

Alexander A. Oliver  
Biomedical Engineering Department  
Michigan Technological University  
Houghton, MI, 49931 USA  
Email: [aaoliver@mtu.edu](mailto:aaoliver@mtu.edu)

## Abstract

Over the past two decades, significant advancements have been made regarding the material formulation, iterative design, and clinical translation of metallic bioresorbable stents. Currently, magnesium-based stent devices have remained at the forefront of bioresorbable stent material development and use. Despite substantial advances, the process of developing novel absorbable stents and their clinical translation is time-consuming, expensive, and challenging. These challenges, coupled with the continuous refinement of alternative bioresorbable metallic bulk materials such as iron and zinc, have intensified the search for an ideal absorbable metallic stent material. Here, we discuss the most recent pre-clinical and clinical evidence for the efficacy of bioresorbable metallic stents and material candidates. From this perspective, strategies to improve the clinical performance of bioresorbable metallic stents are considered and critically discussed, spanning material alloy development, surface manipulations, material processing techniques, and preclinical/biological testing considerations.

Keywords: Bioresorbable Stent; Magnesium; Iron; Zinc; Preclinical Study



## 1. Introduction

Cardiovascular disease is the leading cause of death in the United States [1]. Within the last 40 years, angioplasty combined with the deployment of endovascular stents has become the gold standard for restoring the patency of atherosclerotic arteries. Approximately 430,000 endovascular stents are deployed annually in the United States alone [1, 2]. The early success of stenting procedures to revascularize target lesions allowed for their widespread adoption within interventional cardiology, and subsequently shaped the current framework of intravascular interventional procedures. Initially, bare metal stents (BMS) were produced using inert corrosion resistant materials such as stainless steels, cobalt chromium, and shape memory nickel-titanium alloys. Drawbacks associated with these permanent intravascular implants include late thrombosis, inflammation, and vascular smooth muscle cell hyperplasia leading to in-stent restenosis [3, 4]. Recognizing that these pitfalls were in part due to the chronic presence of the metal meshwork in association with a pro-inflammatory disease environment, extensive efforts have aimed to incorporate antiproliferative drug coatings onto BMS platforms termed drug eluting stents (DES) [5], and also to develop fully bioresorbable polymeric stents [6]. Regardless of BMS or DES deployment, de novo neoatherosclerosis is the primary failure method at very late time points [7-9]. Due to the many complications associated with permanent stents, there has been a major shift towards clinical research and development of completely bioresorbable stents (BRS) [10].

The serious clinical limitations associated with polymeric BRS, which are directly linked to polymer mechanical properties, have been extensively documented [6]. In addition, the presence of polymer in the human body was found to trigger vascular toxicity and local inflammatory response. Consequently, intrinsically high mechanical strength and ductility accompanied by adequate biocompatibility favors metallic candidates for application as a BRS [11, 12]. Magnesium (Mg), iron (Fe), and zinc (Zn) based materials have emerged as the three main classes of candidate metallic BRS materials due to their ability to biocorrode within the body. Additionally, Mg, Fe, and Zn are present endogenously in relatively high concentrations and play many physiological roles. This means that as these materials corrode, their byproducts will avoid provoking systemic toxicity and will rather be safely metabolized and excreted by natural mechanisms [12].

The process of developing novel absorbable stents and their clinical translation is time-consuming, expensive, and challenging. This is particularly true in the case of metallic absorbable stents, which have to retain biocompatibility throughout the degradation process without producing toxic and/or inflammatory responses or generating harmful degradation products [13, 14]. Material modifications for stents typically involves balancing opposed mechanical requirements, which are essential for successful deployment and long-term biomechanical stability. As illustrated in Fig. 1, the expected stent material characteristics are contradictory: high elastic modulus prevents recoil, low yield strength allows stent expansion at low inflation pressures, high tensile properties after expansion provide radial strength and permit the use of thinner struts, high ductility is needed to undergo plastic deformation during expansion without cracking [15, 16]. Beyond the conventional constraints, absorbable stents incur additional design considerations in material selection and modification, such as degradation profile, biocompatibility of by-products, and deterioration of mechanical properties due to degradation. Combining the aforementioned mechanical and degradation properties within the same material is extremely challenging [14].

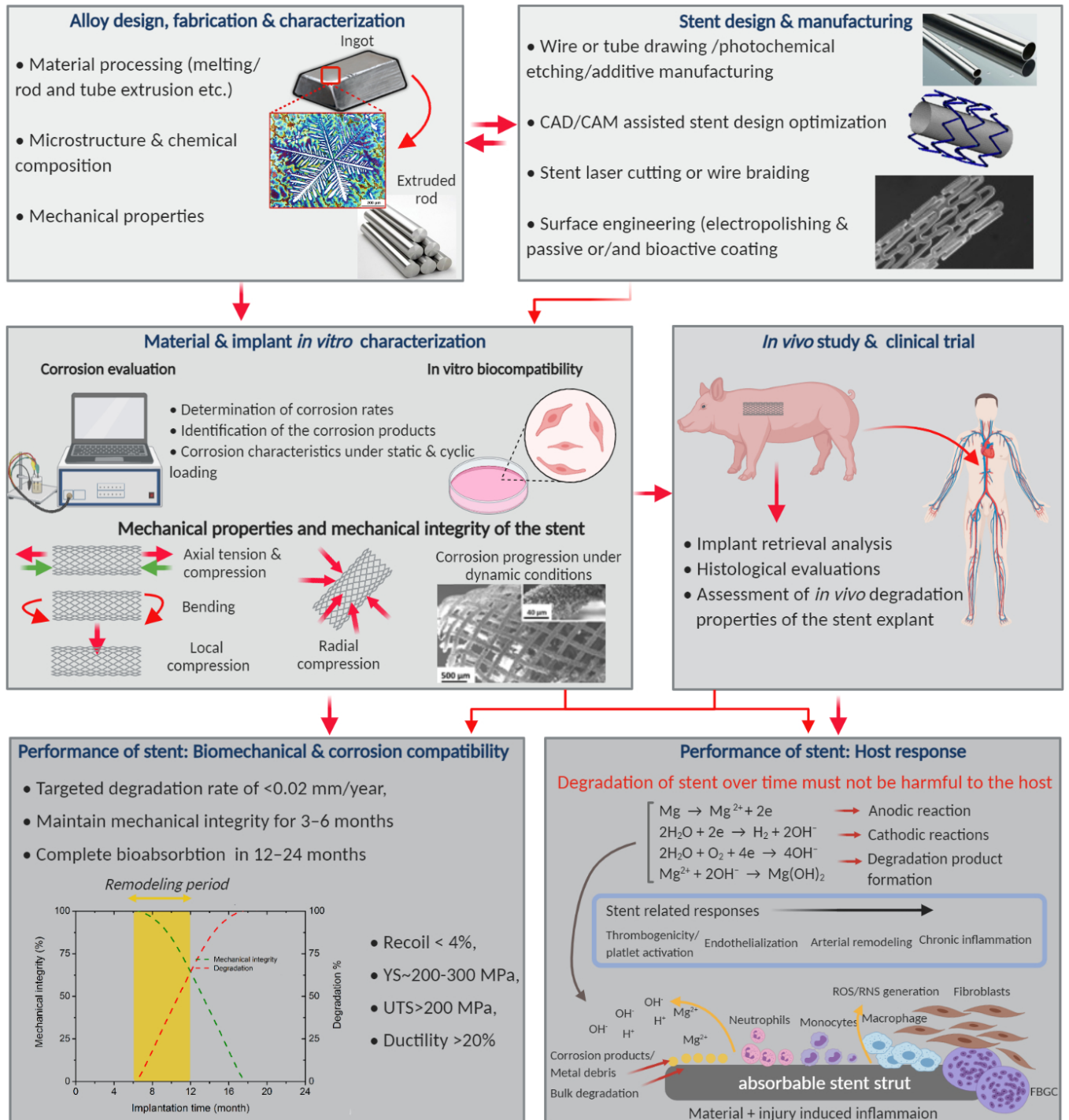


**Figure 1. Development of absorbable cardiovascular stents.** Contemporary endovascular stents are the product of an iterative design and development process that leverages evolving concepts in vascular biology and materials engineering. Stent development process involves (1) the creation of increasingly safer, more reliable, and more physiologically appropriate stent platform material, (2) stent manufacturing (involving design optimization, and surface engineering), (3) *in vitro* corrosion & biocompatibility characterization, (4) *in vivo* animal study & clinical

*trials. Absorbable metallic stent technology matures from iterative approaches to evidence-based strategies, incorporating new knowledge obtained from preclinical and clinical studies. Diagram showing compromise between degradation and mechanical integrity of an ideal stent and the stent micrograph were adapted with permission from Ref. [15], Elsevier Created with BioRender.com*

Before new stents can be introduced to clinical use, many studies are required to prove safety and compatibility (Fig. 1). Although in vitro experiments yield important information on mechanical and corrosion behavior, and general cytotoxicity, they cannot replace the response of a complex organism. For instance, every implanted material evokes a response from the immune system, with the aim of responding to and eliminating the foreign implant. The host response cannot be simulated effectively with in vitro models, solidifying the need for comprehensive in vivo testing. Additionally, the cellular response to biodegradable metals involves complex coordination from cells residing in the particular tissue in question as well as circulating cells; both of which cannot be replicated effectively in vitro. The comprehensive evaluation of biodegradable stent candidate metals requires in vivo implantation studies.

Absorbable Mg, Zn and Fe are challenging to evaluate due to their dynamic interactive surface and continuous degradation that releases a variety of byproducts, continuously changing the device/tissue interface. This dynamic tissue implant interface is of special interest when evaluating biocompatibility, as it is the focal point of contact between cells and tissues with the material and degradation products [17]. Currently, it is encouraging that Mg-based stents have been successfully applied in patients with limited use, and an Fe-based stent clinical trial is in progress on the IBS scaffold. This motivates clinicians and scientists to consider additional absorbable metallic platforms as well as bioactive surface treatments for BRS applications. Since the translation of metallic absorbable stents is multidisciplinary (as depicted in Fig. 1), which involves material design and preparation, medical device design and fabrication, biological evaluation, clinical assessment, and product registration, it is necessary to establish a cooperative platform between universities, institutes, hospitals, and enterprises to facilitate R&D of BRS stents, as well as their preclinical and clinical studies prior to product marketing [18].

Human trials for advanced absorbable metal-based stents have shown a wide variety of clinical efficacies and adverse events. Although a variety of alloys (and surface treatments) for absorbable metallic stents has been developed and investigated in vivo, the ideal absorbable stent material has not yet been discovered [19]. In this review, we describe the state-of-the-art technology in the field of absorbable metallic stents for cardiovascular applications. We focus on recent developments in the context of preclinical testing and clinical translation and describe important advances in the development of novel materials. Here, the strengths, limitations, and modification strategies of BRS materials are critically evaluated and summarized. While most reviews to date in the metallic BRS field focus primarily on material development, this review will focus on the translation of these developments to clinical and in vivo performance. A specific emphasis will be placed on the biological response to BRS materials. Therefore, contributions featuring clinical or in vivo models will be reviewed comprehensively, while in vitro studies will be used as supplementary material.

## 2. Stenting

Balloon angioplasty and stenting is a minimally invasive medical procedure when compared to coronary artery bypass grafting. While restoring blood flow is vital for the patient's survival, expanding the stent against the arterial wall causes widespread damage to the underlying vessel and targeted lesion. The expansion of the balloon and deployment of a stent will denude the endothelial layer, exposing pro-thrombogenic extracellular matrix such as collagen to platelets circulating in the blood [3, 20]. The damage to smooth muscle cells (SMCs) associated with stent expansion elicits a nonspecific inflammatory response and activates vascular SMCs to migrate and proliferate, reducing the luminal cross section. This cellular growth forms into a neointimal tissue protrusion that often occludes the lumen, a process known as restenosis [21, 22].

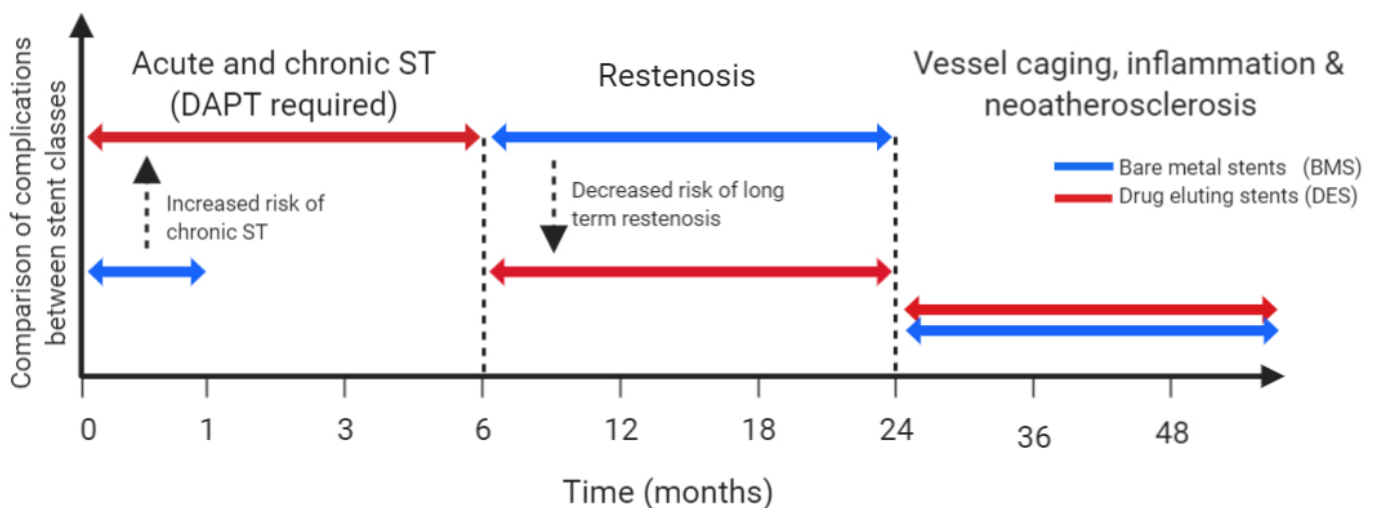


**Figure 2.** Generalized complications associated with BMSs and DESs over time (the higher value the higher probability of complications). Both BMS and DESs suffer from similar failure modes at long term implantation, related to the chronic presence of the scaffold material. DAPT: dual antiplatelet therapy, ST: stent thrombosis Created with BioRender.com

The endothelium plays a critical role in regulating the biological response to stents [23]. As denudation of the endothelium is unavoidable when implanting stents, the rate at which the vessel wall and stent struts can reendothelialize is vital for the implant's success. Indeed, stent strut thickness and geometry must be carefully considered to streamline the hemodynamics in order to improve the rate of reendothelialization, which can ultimately reduce rates of restenosis [24-26]. Vessel walls and stent struts without the protection of a confluent endothelium are at a notably higher risk for thrombus formation [27]. Endothelial cells (EC) also play an important role in regulating neointimal tissue formation, as EC

dysfunction may lead to excessive leukocyte recruitment and SMC proliferation around the stent struts [23]. The injury associated with stent implantation and the presence of foreign material will lead to the recruitment of circulating leukocytes. As part of the foreign body response, these inflammatory cells will attempt to contain, neutralize, or remove the implant. Although inflammation is essential for the artery to heal, high degrees of inflammation worsen the restenosis response [28, 29]. This is because a pro-inflammatory environment will increase the degree of neo-intimal SMC migration and proliferation [30]. For BMSs, SMC hyperplasia is the leading cause of restenosis and failure [31].

1<sup>st</sup> generation DESs were introduced to reduce rates of restenosis associated with balloon angioplasty and stent deployment and were subsequently replaced with safer 2<sup>nd</sup> and 3<sup>rd</sup> generation DES. Critically, DES succeeded in dramatically reducing restenosis rates caused by the nonspecific tissue injury response, yet introduced new problems. Due to delayed healing of the endothelium caused by unintended inhibiting effects of the eluting drug, struts of the implanted DES remain uncovered, elevating acute and chronic stent thrombosis rates for DES as per the red line shown in Fig. 2. BMS also suffer from acute stent thrombosis, but on a time scale of 14-30 days after implantation, as compared to the ~6 month endothelial dysfunction period for DES [32]. Due to the lethality of stent thrombosis, dual antiplatelet therapy (DAPT) is recommended for at least 30 days for BMS, and a minimum of 6 months for DES, with time frames extending up to 2 years for DES [32, 33]. Although effective at decreasing overall complications of percutaneous coronary interventions (PCI) and stent implantations, DES are recommended to patients who can complete a minimum 6 month course of DAPT, who satisfy comorbidity risk factors such as diabetes and chronic kidney disease, and who possess complex lesion characteristics. The overall selection of BMS vs. DES in the clinic relies on extensive patient work up, and is evaluated on a case by case basis [32, 33].

Due to the injury response from balloon angioplasty and stent deployment, newly engineered degradable metal stents must support healthy reendothelialization, prevent or avoid excessive inflammation, and avoid worsening the natural SMC hyperplasia response during the life time of the degradable stent (~ 2 years). If successful, BRS could alleviate the common late term failure modes of both BMS and DES, which include persistent inflammatory responses, very late stent thrombosis, and neoatherosclerosis [6, 7]. This could be of exceptional importance given the fact that PCIs are being used in younger patients, with an expected prognosis greater than 15-20 years of life.

### 3. Mg stents in the clinic

#### 3.1 Early use of BRS Mg in the clinic

Ref	Stent	Condition	Endothelialization	Vessel Performance	Inflammation	Clinical Outcome and Conclusions
[34, 35]	AMS (Biotronik)	Inadvertent ligation of pulmonary artery	Histology at 5 months demonstrated complete endothelialization. NI luminal cells + for VWF	Stent maintained patency of left pulmonary artery for 5 months, and completely dissolved. NI formation up to 100µm thick	Immunostaining demonstrated that the NI was composed of SMCs and no inflammatory cells were observed	Stent was able to maintain patency of artery until it completely dissolved without eliciting any notable negative biological responses
[36]	AMS	Critical coarctation	No Data	Recatheterization revealed a decrease in diameter of the stented area, leading to a 2nd stent being implanted	No Data	The first stent lost mechanical integrity by 15 days. Despite the use of 2 stents, no pathological levels of Mg were detected in the serum of the patient
[37]	MAGIC EXPLORER (Biotronik)	Stenotic aorto-pulmonary collateral	No Data	Significant restenosis by 4 month follow up	No Data	Stent was able to immediately restore patency. Significant restenosis was observed by 4 months

**Table 1:** Brief summary of first in patient single device investigations for Mg based BRS's. NI: neointima, VWF: Von Willebrand factor

Ref	Stent	Trial	Clinical Performance	Limb Salvage Rate
[38]	AMS	Preliminary study for AMS INSIGHT clinical trial - 20 patients with chronic limb ischemia received AMS stent(s) in infrapopliteal arteries.	% Stenosis measured via duplex doppler ultrasound. At discharge, 18 patients had normal blood flow (<20% stenosis) and 2 had 30-40% stenosis. At 1 month, 17 of the 19 surviving patients had 0% stenosis, 1 had 20-30% and one had 60-70%. At 3 months, 13/19 patients had normal blood flow, 4 had partial stenosis, and 2 had complete occlusion.	100%
[39]	AMS	12 month follow up for AMS INSIGHT preliminary trial	CFDU revealed significant restenosis in 3 patients after 85, 107, and 181 days respectively.	95%
[40]	AMS	AMS INSIGHT - (n = 74) implanted into the infrapopliteal arteries of patients with chronic limb ischemia (>50% stenosis) compared to just percutaneous transluminal angioplasty (PTA) (n = 75) of patients with same conditions	At 6 month follow up, binary restenosis rate (>50% diameter stenosis) and late lumen loss was significantly higher for the BRS group.	By 1 month, 2 patients in each group received an amputation (2/50 4% for PTA) and (2/59 3.4% for BRS).

**Table 2.** Clinical Mg BRS trials in treatment of peripheral artery disease.

Mg based BRS first entered clinic practice on a case by case basis for pediatric applications. Reports from these cases are summarized in Table 1. Zartner et al. reported the use of a Mg alloy BRS to successfully treat an inadvertent ligation of the left pulmonary artery [35]. The stent maintained patency of the left pulmonary artery until it completely degraded. Histology at 5 months revealed complete reendothelialization of the stented area without apparent calcification, necrosis, or structural damage to the arterial wall. The dissolved stent struts had been replaced with a crystalline calcium phosphate material. Immunostaining revealed a neointima composed of SMCs ( $\alpha$ -SMA+ cells) without observation of inflammatory cells (CD68+, CD3+, CD79+, or MAC+ cells) at the implant-tissue interface. Complete degradation of the stent led to minimal changes within the vessel wall [34]. Schranz et al. reported the use of a Mg based BRS to successfully treat critical coarctation in a newborn [36]. The stent lost mechanical integrity after 15 days due to corrosion, requiring a second BRS implantation. Following substantial degradation of the two stents, no pathological levels of Mg were detected in the newborn. McMahon et al. reported less favorable results after they implanted a Mg based BRS into a stenotic aortopulmonary collateral artery of a two month old [37]. Although the stent was able to immediately restore patency with no adverse effects, significant restenosis was seen at the 4 month follow up. These initial investigations generated interest to further develop BRS, although it was generally accepted that the corrosion rate was too high.

### 3.1.2 Mg based BRS clinical investigations

The first preclinical trial was reported by Peeters et al. who implanted Absorbable Metal Stents (AMS) (Biotronik, Berlin, Germany) into the infrapopliteal arteries of 20 patients with critical limb ischemia (CLI) [38]. Late lumen loss as a result of intimal hyperplasia is a major concern for stented small diameter vessels such as the infrapopliteal arteries, which makes BRS an attractive option for this application. The AMS was a Mg alloy stent with a 165 $\mu$ m strut thickness composed of 93 wt% Mg and the balance rare earth elements[41].

A perfect procedural success rate (procedural success defined by no adverse events and < 30% residual stenosis via angiography) and limb salvage rate at both the 3 and 12 month follow ups suggested promising potential for Mg based BRS use in the clinic [38, 39]. However, the degree of restenosis at both 3 and 12 month follow ups suggested that the AMS would benefit from improved mechanical strength and/or a decreased corrosion rate [39].

The preliminary findings reported by Peeters et al. and Bosiers et al. resulted in the AMS INSIGHT trial, which evaluated the performance of Biotronik AMS stents (n = 74) to treat CLI in infrapopliteal atherosclerotic lesions (>50% stenosis) relative to percutaneous transluminal angioplasty (PTA, the standard treatment) (n = 75) [40]. Procedural success was 100% for the Mg based BRS as opposed to 96% for PTA. By the 6 month follow up, significantly fewer arteries maintained <50% patency in the stent group versus the PTA group. In comparison to contemporary stents used to treat CLI, the binary restenosis rate (>50% stenosis) for the AMS was 68.2% as compared to 55.3% and 39.1% for standard permanent BMS and 4% and 0% for standard DES's in infrapopliteal arteries at 6 months follow up, as

**Table 3.** Clinical trials - treatment of coronary artery disease

Study	Stent	Trial	Vessel Performance	Target Lesion Failure <sup>1*</sup>	Clinical Outcome and Conclusions
[43]	AMS	PROGRESS AMS: 63 patients received AMS stents to treat lesions of 50-99% stenosis in coronary arteries	4 month follow up revealed significant restenosis. IVUS revealed decrease of external elastic membrane volume contributed to 42% of the restenosis and neointimal formation to 45%.	TLF rate was 24% (15/63) at 4 months, all were CD-TLR. Between 4 and 12 months, 2 more CD-TLRs occurred, for a cumulative 27% TLF rate	Notable restenosis due to vessel recoil and neointimal formation suggested the AMS should be engineered to possess improved mechanical strength/slower corrosion rate, and would likely benefit from a drug eluting coating
[44]	AMS	Followed 8 patients from PROGRESS AMS from 12 to up to 28 months	No late developments of neointimal formation or stent recoil. In stent diameter stenosis and late lumen loss actually improved from 4 month to late (12 - 28 month) time points	No data	Although short term performance of AMS was not ideal, late follow ups demonstrate positive remodeling after significant stent degradation
[45]	DREAMS (Biotronik)	BIOSOLVE-1: 46 patients had stents implanted in coronary arteries with lesions of 50-99% stenosis	By angiography, a significant amount of diameter stenosis was observed at 6 months, however it slightly improved by the 12 month follow up. IVUS revealed that at 6 months, late lumen loss was as a result of 73% reduction in scaffold cross sectional area and 27% neointimal hyperplasia. At 12 months, it was 69% and 31%, respectively.	At 6 months, 4% (2/46) had TLF (both CD-TLRs), which rose to 7% (3/43) by 12 months, as one patient had periprocedural TVMI that occurred during angiography at 12 month follow up	TLF rate was comparable to industry standard DESs. However, the late lumen loss for DREAMS was not comparable to industry standards. Therefore, the results demonstrated the BRS could be further improved to reduce stent recoil and neointimal hyperplasia
[46]	DREAMS	BIOSOLVE-1: 3 year follow up	7 patients had angiographic follow up at 28±4 months. In scaffold late lumen loss improved from 0.51±0.46mm at 12 months to 0.32±0.32mm. Late lumen loss improved relative to BIOSOLVE-1/DREAMS 1G. IVUS revealed a decrease in neointimal area from 0.30 mm <sup>2</sup> for DREAMS 1G to 0.08mm <sup>2</sup> for DREAMS 2G. In scaffold late lumen loss at 6 months also decreased from 0.65 mm for BIOSOLVE-1/DREAMS 1G to 0.44 mm from BIOSOLVE-2/DREAMS 2G)	No additional TLFs occurred between 1 and 3 years	This study demonstrated great long term safety rates of DREAMS 1G and lumen gain at the 3 year time point after the stent is dissolved.
[47]	DREAMS 2G(Biotronik)	BIOSOLVE-2: 123 patients received DREAMS 2G into coronary arteries with of 50-99% stenosis	BIOSOLVE-2: 123 patients received DREAMS 2G into coronary arteries with of 50-99% stenosis	3.3% (4/123) TLF rate at 6 months (one patient had cardiac death, one had a periprocedural TVMI, and 2 had CD-TLR)	Improved performance relative to DREAMS 1G in the BIOSOLVE-1 trial.
[48]	DREAMS 2G	BIOSOLVE 2: Up to 12 month follow up	In scaffold late lumen loss and diameter stenosis remained consistent from 6 to 12 months.	No TLF events occurred between 6 and 12 months	Safety and performance of DREAMS 2G stents is sustained from 6 to 12 months
[49]	DREAMS 2G	BIOSOLVE-2: Up to 12 month follow up	By OCT of 65 patients, mean and minimum lumen area significantly decreased from post procedure to 6 months. However, these values remained relatively constant (even slightly improved) from 6 to 12 months.	No new data	Restoration of vessel geometry and vasomotion were demonstrated at 12 months post implantation, while preserving lumen size between 6 and 12 months.
[50]	DREAMS 2G & Magmaris	Same as above but 3 year follow up	Late lumen loss slightly increased from 12 to 36 months (0.39±0.27 mm to 0.54±0.38 mm) for the BIOSOLVE 2 trial	One additional CD-TLR occurred in the BIOSOLVE 2 group by the 3 year follow up, for a final TLF rate of 6.8% (BIOSOLVE 2 only)	TLF rates very comparable to contemporary DESs for up to 3 years
[51]	Magmaris (Biotronik) for BIOSOLVE-3	BIOSOLVE-3: 61 patients with same conditions as previous BIOSOLVE studies. BIOSOLVE-2 and BIOSOLVE-3 results pooled together. Evaluation at 12 months	By angiography, late lumen loss at 12 months was essentially the same between BIOSOLVE-2 and BIOSOLVE-3 (in scaffold late lumen loss of 0.39±0.27 mm for DREAMS 2G versus 0.39±39 mm for Magmaris).	At 6 months, TLF rate of pooled BIOSOLVE-2 and BIOSOLVE-3 was 3.3% (two cardiac deaths, one TVMI, three CD-TLR). It was 3.3% (2/61) for BIOSOLVE-3 exclusively. No additional TLFs were observed between 6 and 12 months for either group	BIOSOLVE-3 provided further evidence to support the promising potential of DREAMS 2G/Magmaris
[52]	DREAMS 2G & Magmaris	Same as above but 2 year follow up	No data	At 24 months, one additional cardiac death and two more CD-TLRs occurred, for a final TLF rate of 5.9%	DREAMS 2G/Magmaris was able to demonstrate sustained safety by exhibiting comparable TLF rates to contemporary DESs at 24 months
[53]	Magmaris	Preliminary study for MAGSTEMI: 20 patients received Magmaris stents to treat ST-segment-elevation myocardial infarction	No data	0% at 30 days. Patients were followed from a range of 59-326 days (median 153 days). Only one CD-TLR occurred at 102 days.	Preliminary trials of Magmaris use to treat STEMI appear to be promising and warrant further study

[54]	Magmaris	MAGSTEMI: Compared Magmaris (n = 74) to Orsiro (n = 76, industry standard DES with same coating) to treat ST-segment-elevation myocardial infarction	Magmaris group had significantly less immediate post implantation in stent lumen gain and significantly higher late lumen loss and diameter restenosis rates at 12 month follow up	By the 12 month follow up, Mg group TLF rate was significantly higher (17.6%, (13/74)) versus the DES control (6.6%, 5/76)	Magmaris was outperformed by the standard DES Orsiro. Magmaris needs to be further improved to reduce vessel recoil (increase radial strength and potentially decrease corrosion rate)
[55]	Magmaris	BIOSOLVE-4: First cohort of 1075 patients with 1121 lesions. Coronary lesions with 50-99% stenosis	No data	According to Kaplan-Meier estimator, TLF rate at 12 months was 4.3% (n = 45) due to 0.2% cardiac death, 1.1% TVMI, and 3.9% CD-TLR.	Estimated TLF values suggest great clinical performance

---

<sup>1</sup> Target Lesion Failure (TLF) is defined as a composite between cardiac death, target vessel myocardial infarction (TVMI), and clinically driven target lesion revascularization (CD-TLR)[42] D.E. Cutlip, S. Windecker, R. Mehran, A. Boam, D.J. Cohen, G.-A. van Es, P. Gabriel Steg, M.-a.l. Morel, L. Mauri, P. Vranckx, Clinical end points in coronary stent trials: a case for standardized definitions, *Circulation* 115(17) (2007) 2344-2351..

OCT: optical coherence tomography, STEMI: ST-segment-elevation myocardial infarction

reported by two separate studies [56, 57]. The authors attributed the suboptimal restenosis of the AMS to stent recoil as a result of the stent corroding too fast and insufficient radial strength. The reports of Mg based BRS use to treat CLI are summarized in Table 3.

The results of the first clinical trial that evaluated the safety and efficacy of Mg based BRS in the coronary arterial environment were published by Erbel et al. in 2007 [43]. The trial, entitled PROGRESS-AMS, consisted of 63 patients who received Biotronik AMSs to treat lesions with 50-99% diameter coronary artery stenosis. All patients achieved procedural success (defined as over 50% reduction of stenosis without major adverse cardiac events before patient discharge) and no acute thrombosis was observed in any patients. However, significant restenosis was observed at the 4 month follow up due to equal contributions of a decrease in external elastic membrane-volume and neointima formation. Although the late lumen loss by 4 months was not optimal, Ghimire et al. reported that at 4 months the degradation of stents in the PROGRESS AMS trial led to a significant increase in vasomotion of their host coronary arteries relative to traditional permanent stents [58]. By one year, major adverse cardiac events (defined as a composite of cardiac death, Q-wave myocardial infarction, or clinically driven target lesion revascularization) were reported in 26.7% of patients. For reference, traditional BMS and DESs had major adverse cardiac event rates of 28% and 6% respectively at 12 months for the same device application [59]. Waksman et al. followed 8 patients from the PROGRESS AMS trial for up to 28 months after the stents had completely dissolved [44]. Their findings demonstrated no late developments of neointimal formation or stent recoil. Interestingly, they reported that in stent diameter stenosis and in stent late lumen loss actually improved from 4 months relative to their very late (12-28 month) follow ups. In summary, the PROGRESS AMS clinical trial served as a proof of concept for Mg based BRS by demonstrating effective deployment and safe corrosion in the atherosclerotic coronary artery environment. Partial corrosion of the BRS at 4 months resulted in improved vasomotion and complete bioresorption led to positive arterial remodeling at very late time points. However, a decrease of external elastic membrane volume is observed at 4 months, likely due to lack of mechanical integrity and stent recoil, demonstrating that the next generation of Mg alloy BRS should be further developed to possess increased mechanical properties and/or a slower corrosion rate. Additionally, the degree of neointimal development and rate of major adverse cardiac events suggested that Mg based BRS could benefit from a drug eluting coating. Therefore, although bare metal Mg alloy stents exhibit excellent biocompatibility in animal models of healthy coronary arteries, the first clinical trial pointed towards the need for a drug eluting coating to achieve acceptable clinical outcomes in the diseased arterial environment of human patients. Indeed, this study motivated engineers and scientists to develop drug eluting coatings for Mg based BRS [60, 61]. Reports related to the results of the PROGRESS AMS clinical trial are summarized in Table 3.

### 3.1.3 Improvements on AMS

Motivated by the results of the AMS INSIGHT and PROGRESS AMS trials, Biotronik further developed their Mg based BRS to improve the strut geometry and reduce the degradation rate through alloying [45]. The second-generation Mg based BRS, entitled "DREAMS" (Drug Eluting Absorbable Metal Scaffold), featured a paclitaxel eluting polylactic-coglycolic acid degradable coating, which is a DES industry standard drug delivery system [62, 63]. The DREAMS was evaluated in the BIOSOLVE-1 clinical trial, where 46 patients with 50-99% diameter coronary artery stenosis were treated with DREAMS implants. As with the PROGRESS AMS trial, all patients achieved procedural success (defined by <30% diameter stenosis without adverse cardiac events) and no scaffold thrombosis was observed. Significant restenosis was observed at 6 months, which was mostly the result of a reduction in scaffold cross sectional area. Neointimal

hyperplasia also contributed to the restenosis, but to a lesser degree than for the AMS, due to the DREAMS drug eluting coating. Diameter stenosis slightly improved from 6 to 12 months as the stent degraded and was absorbed, as the contributions of scaffold cross sectional area reduction and neointimal hyperplasia to late lumen loss remained consistent. The consistency between the 6 and 12 month follow ups demonstrated no chronic recoil, negative remodeling, or excessive late neointimal hyperplasia. The rate of target lesion failure (TLF) (composite of cardiac death, target vessel myocardial infarction, and clinically driven target lesion revascularization – referred to as major adverse cardiac events in PROGRESS AMS) for the DREAMS trial drastically improved to 4.7% from 26.7% for the AMS. Seven patients had very late follow ups (28±4 months), which revealed similar findings to the late follow ups for the PROGRESS AMS trial [46]. For DREAMS, in-scaffold late lumen loss improved from 12 months to the very late follow ups and no additional TLFs occurred. Although the TLF rate was very promising and comparable to industry standard DESs, the degree of late lumen loss exhibited by DREAMS at 6 months was significantly greater than industry standard DESs. This suggested that the Mg based BRS should be further improved to reduce recoil and neointimal hyperplasia within the first 6 months.

Biotronik developed a second generation drug eluting Mg based BRS, entitled DREAMS 2G, which featured an improved strut design to increase radial force and flexibility [47]. DREAMS 2G possessed a sirolimus eluting poly-L-lactide coating, which is the same coating as the commercially available Orsiro DES that has demonstrated promising clinical results [64]. DREAMS was evaluated in the BIOSOLVE-2 clinical trial where 123 patients received DREAMS 2G into coronary artery lesions with 50-99% diameter stenosis [47]. In similar fashion as its predecessors, DREAMS 2G exhibited great procedural success and TLF rates, but also significant restenosis by 6 months. Late lumen loss was attributed to both neointimal hyperplasia and late scaffold recoil [65]. However, late lumen loss for DREAMS 2G had improved relative to DREAMS 1G and AMS, largely due to a decrease in neointimal area. The 12 month follow up revealed that late lumen loss and diameter stenosis remained relatively consistent and no additional TLFs occurred from 6 to 12 months [48]. Garcia-Garcia et al. reported that the host vessels exhibited restoration of vessel geometry and vasomotion with the degradation of the DREAMS-2G at 12 months [49]. Twenty five patients from the BIOSOLVE-2 trial volunteered for a 36 month follow up, which revealed that the late lumen loss and diameter stenosis stayed slightly increased from 12 to 36 months [50].

Due to the success of the BIOSOLVE-2 trial, the DREAMS-2G was remarketed under the name “Magmaris” and evaluated in the BIOSOLVE-3 clinical trial, wherein Magmaris stents (n = 61) were deployed under the same conditions as the previous BIOSOLVE trials [51]. By angiography, late lumen loss at 12 months was essentially identical between BIOSOLVE-2 and BIOSOLVE-3. With the BIOSOLVE 2 and 3 results pooled together (n = 189), the Mg based BRS experienced an exceptional 12-month TLF rate, which was very comparable to the TLF rate of the Orsiro stent (BIOFLOW-2 trial), a permanent drug eluting stent from Biotronik [66]. Another promising finding was that imaging with optical coherence tomography (OCT) revealed no malapposed struts at 6 or 12 months. At the 2 year follow up, no probable or definite thrombosis was observed and the TLF rate was 5.9% [52]. For reference, the TLF rates in comparable studies of industry standard Everolimus eluting CoCr alloy stents were 3.8%, 3.0%, 7.9%, and 8.9% as reported by four separate studies, respectively [67-70]. Considering the Mg based BRS was designed to completely absorb after 12 months, the positive findings at 2 years demonstrate clinical safety after the stent has completely absorbed. Indeed, at the 3 year follow up, only one more case of TLF occurred, for a final rate of 6.3% [71]. Yuichi et al. recently contributed a comprehensive review of the performance of

DREAMS 2G/Magmaris in the BIOSOLVE clinical trials relative to previous clinical trials that evaluated the performance of polymeric BRS [72].

Inspired by the success of the Magmaris stent in the BIOSOLVE-2 and BIOSOLVE-3 trials, the MAGSTEMI clinical trial was launched, which investigated the safety and efficacy of Magmaris stents to treat patients with ST-segment-elevation myocardial infarction (STEMI). A preliminary study, reported by de Hemptinne et al., implanted Magmaris stents into 20 patients [53]. The preliminary results were very promising, as there was only one case of TLF by the last follow up, which ranged from 59 to 326 days. In the full MAGSTEMI clinical trial, 74 patients received Magmaris stents and 76 patients received Orsiro stents (Permanent DES with same drug eluting coating as Magmaris) to treat STEMI [54]. The Magmaris stent caused significantly less immediate post implantation in-stent lumen gain. Additionally, by the 12 month follow up, the Magmaris group had significantly higher late lumen loss and diameter stenosis, as well as a notably higher TLF rate compared to the Orsiro group. The reports from the BIOSOLVE clinical trials are summarized in Table 3.

#### 3.1.4 Current clinical investigations

In response to the results of the clinical trials, Fajadet et al published a census paper for recommended use of the stents upon commercial launch [73]. The stents were recommended for use in patients with discrete short lesions and a life expectancy greater than 5 years, who are suspected to benefit from regained vasomotion following the absorption of the stent. Although recommended commercial use of the Magmaris stent demonstrates progress in the field of metallic BRS, there remain major limitations. When the performance of Magmaris in the BIOSOLVE trials is compared to the Orsiro DES to treat patients under the same conditions, post procedure diameter stenosis is significantly greater for Magmaris ( $11.7\pm 5.2\%$  for Magmaris vs  $4.9\pm 7.5\%$  for Orsiro,  $p < 0.001$ ). This is likely due to the reduced mechanical integrity of the Magmaris stent relative to Orsiro even though Magmaris had an original strut thickness of  $150\ \mu\text{m}$  as opposed to  $60\text{-}80\ \mu\text{m}$  for the Orsiro [74]. These findings corroborated with the results of the MAGSTEMI trial. Indeed, there are case reports of Magmaris failure due to mechanical inadequacies [75-77]. The inferior mechanical properties of Magmaris relative to contemporary stent materials limit its use to short, less calcific lesions in cases where the patient has much to gain from the complete resorption of the stent (i.e. they are young and otherwise healthy).

The BIOSOLVE-4 clinical trial, which is currently still in progress, is evaluating the post market performance of Magmaris stents to treat coronary lesions with 50-99% stenosis [55]. The first cohort of 1075 patients with 1121 lesions exhibited a great procedural success rate and a promising TLF rate consistent with contemporary DESs. These results have been summarized in Table 3. So far, the BIOSOLVE-4 trial appears to demonstrate great safety ratings for the Magmaris stents to treat simple lesions. The second cohort of the BIOSOLVE-4 trial is still in progress and will increase the patient size to 2054 patients. The BIOSOLVE-4 clinical trial will serve as a comprehensive post market surveillance of the Magmaris stent to treat patients with symptomatic CAD and single de novo native coronary artery lesions [78].

#### 3.2 New Strategies to improve Mg Performance

The introduction of Mg-based absorbable stents was one of the most important innovations in the continuously evolving field of bioresorbable stents. Although very promising, the initial experience with absorbable Mg stents has raised concerns including fast degradation and excessive release of Mg ions and  $\text{H}_2$  gas. In addition, structural and mechanical integrity of Mg stents in physiological solutions over time

has not yet met expectations. Ongoing development in Mg alloys design and processing might resolve these problems. Many investigations have been carried out in an effort to increase the control of Mg biodegradation, both in exploration of new alloys and manufacturing strategies and developing surface modifications and coatings as illustrated in Fig. 3.

By meticulous control of alloy formulation, and microstructural design, significant progress has been made in the development of biocompatible high strength Mg-based alloys with acceptable ductility. Alloying with Ca, Mn, Zn, Sn, Al, Zr, Sr as well as rare earth elements not only increases the mechanical strength through promotion of different strengthening mechanisms but also leads to improved corrosion performance. For instance, a high-strength, low-alloy, high-purity Mg-Zn-Ca alloy has been developed that exhibits high mechanical properties due to the promotion of grain size refinement and precipitation strengthening, together with a slow degradation rate [79, 80]. The reduced corrosion rates and homogenous surface dissolution results from the tailored composition and refinement and redistribution of the intermetallic particles, which leads to formation of anodic second phase particles instead of cathodic ones. Another approach to simultaneously improve the mechanical properties and corrosion behavior is to decrease the grain size by severe plastic deformation techniques (SPD), leading to the formation of ultra-fine-grained materials [81, 82]. While significant effects of grain refining on the corrosion behavior have been reported for Mg in standard electrolytes, only a few studies can be found related to the biomedical applications of SPD processed Mg stents. Regarding the corrosion behavior, the decrease in size of second phase particles and the resulting increase in microstructural homogeneity contributes to remarkably reduced localized corrosion [83]. Moreover, Mg-based bulk metallic glasses have been of interest as prospective materials for biodegradable implants [83]. Due to their homogeneous, single-phase amorphous nature, they exhibit good mechanical properties and are less susceptible to localized corrosion than their conventionally processed counterparts [84].

New manufacturing techniques are also currently under development. One of the key difficulties concerning the assessment of alloy performance is the complexity of producing prototype stents. The use of flat sheet precursors instead of tubular ones can be combined with convectional laser cutting to produce inflatable stent meshes. Such manufacturing routes can be highly advantageous for testing new Mg-alloys combined with more realistic geometries [85]. Additive manufacturing (AM) techniques, especially selective laser melting (SLM), have raised significant attention for producing biodegradable implants [86]. Mg has very low melting and boiling points (905 K and 1363 K respectively) rendering melting based AM processes such as SLM highly unstable due to the vapor accumulation and laser beam diffraction. The high reactivity of the material combined with the micrometric powder feedstock generates safety issues [87]. The research has been mainly focused on the processability, where with optimized machine architectures [88], the geometrical flexibility of SLM could be exploited along with the enhanced mechanical properties owing to the fast cooling rates of the process [89]. If further developed, AM could eventually be a powerful tool for Mg processing in BRS. Areas of interest include better corrosion control, and the use of patient specific dimensions which would allow for customizable Mg BRS devices.

- Limitation of Mg-based absorbable stents**
- Rapid degradation in physiological environment
  - Reduced mechanical integrity due to rapid dissolution
  - Excessive release of H<sub>2</sub> and degradation products
    - Non-homogenous, localized corrosion

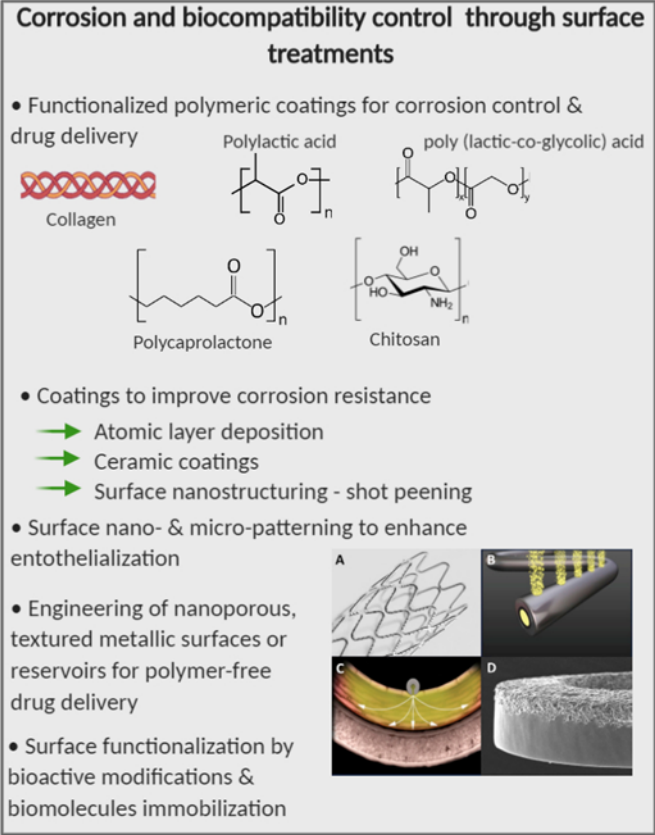
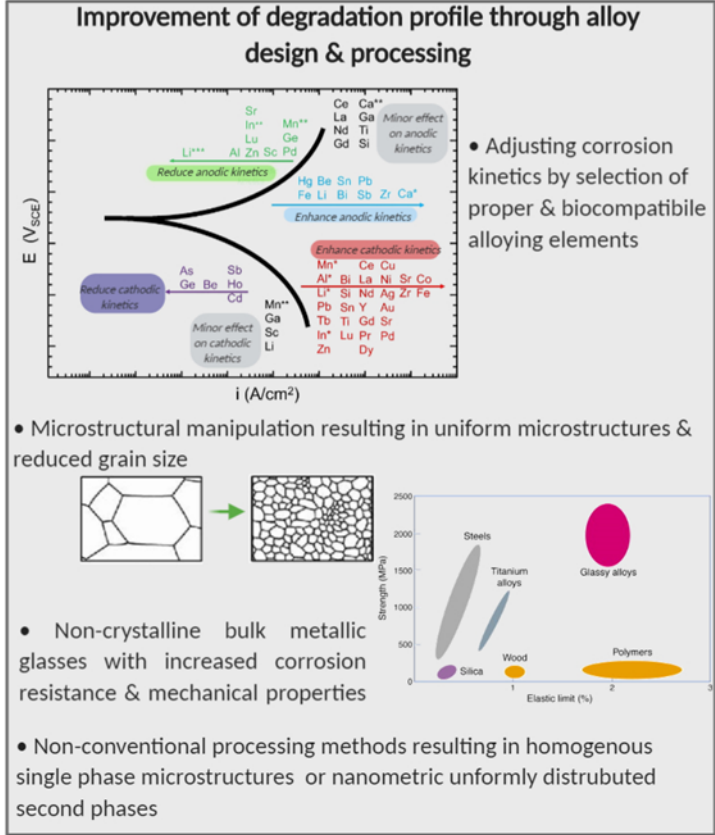


**Figure 3.** Limitations of Mg-based absorbable stents and the development strategies to overcome them including material development and surface engineering. Selection of alloying elements for corrosion control and bulk metallic glasses mechanical properties diagrams adapted with permission from references [90] and [91], Surface Engineering for polymer free delivery adapted with permission from reference [92] Elsevier. Created with BioRender.com

Coatings in absorbable Mg stents have been the focus of recent attention in order to control the degradation kinetics and improve the interaction between the implant and host. In terms of the biological response, the proliferation of endothelial cells is desired to avoid thrombus formation [93]. Drug eluting Mg-based stents coated with polymers (PLLA, PLGA) displayed better performance when compared to Mg BMS in clinical studies. However, the application of polymer for drug elution contributes to DES failure by triggering vascular toxicity and local inflammatory responses [92]. Polymer-free metallic stents where nanoporous or textured metallic surfaces or drug reservoirs are used for drug carriage are being developed as an alternative approach [94, 95]. Randomized trials using polymer-free DESs have shown promising outcomes, however long-term follow-up on a large population is required to assess whether this strategy has clear advantages over polymer coated DES. Kang H. M. et al. recently investigated the feasibility of the novel asymmetrical coating technique on Mg providing an anti-proliferative effect abluminally without affecting luminal endothelialization. They found that sirolimus loaded

PLGA/poly(ether imide) (PEI) coating on abluminal surface suppressed restenosis response, while PEI on the luminal surface substantially lowered the corrosion rate of WE43 stent [96].

In response to surface modifications on Mg substrates, enhanced adhesion of cells alone is not sufficient for appropriate endothelial expression of antithrombogenic markers. An endothelial layer in an activated state loses its protective effect by expression of a pro-coagulant and pro-inflammatory phenotype with downregulated thrombomodulin, nitric oxide (NO) synthesis and reduced heparan-sulfate, while up-regulating ligands for platelet and leukocyte adhesion [97]. The investigation of surface topography could benefit the phenotypic modulation of endothelial cells because some topographies promote physiological endothelial cell function (secretion of extracellular matrix proteins, NO, Prostaglandin, etc.) [98]. Despite improvements in the materials used for resorbable stent platforms and tailoring their surface properties, patients with cardiovascular diseases still require antithrombotic therapy with anticoagulants, antiplatelet agents or both to reduce the risk of thrombosis [32, 92]. Strategies for biomolecule immobilization, in situ regenerating bioactive modifications and on-demand release systems are new directions for the development of smart, responsive absorbable stent surfaces with an extended bioactivity span. These novel trends target specific molecules in biological pathways as compared to current non-specific approaches that are based on anti-proliferative drug eluting coatings [99].

## 4. Progress of alternative bulk materials; Fe and Zn based stents

Clinical trials featuring Mg based BRS have demonstrated high procedural success and safety rates accompanied by exceptionally low rates of in- scaffold thrombosis and strut malposition (Table 3). However, Mg based BRS will require a drug eluting coating to mitigate neointimal formation, which will likely lead to negative side effects such as delayed endothelialization and the need for a prolonged dual antiplatelet therapy for the patient (>6 months). Overall, key problems with Mg stent biocompatibility from past in vivo studies appear to be mechanically related. The rapid degradation time and scaffold disappearance results in higher vessel recoil and late lumen loss when compared to its leading DES counterparts. Additionally, Mg alloy stents may not be able to match the strength of traditional stent materials, resulting in more acute and late recoil, limiting their application to shorter, less calcific lesions. The lower radial strength of Mg materials necessitates larger struts, which dramatically reduce maneuverability and increase arterial wall injury upon deployment. The use of stronger bulk materials such as Fe or alloyed Zn could result in benefits over Mg-based materials. The attention over Fe and Zn based stents has been growing in the last decade, although they have not yet achieved the clinical maturity as their Mg based counterparts. Hence, the literature is limited to biocompatibility concerns and clinical translation, which are further analyzed in the following sections.

### 4.1 Fe based materials

#### 4.1.1 Early in vivo examination

Chronologically, Fe based stents were the first metallic BRS to be fabricated and evaluated in vivo [100], likely due to their superior mechanical properties relative to other biodegradable metals and relatively easier manufacturing of the tubular precursor and laser cutting. Early experiences with Fe based stents in animal models demonstrated a mild to moderate inflammatory response with a high degree of variability within and between samples [100-102]. As is typical with foreign body reactions, the initial peri-implant tissue was mainly composed of lymphocytes and granulocytes, with macrophages slowly becoming the predominate cell type over time and the occasional presence of multinucleated foreign body giant cells.

No tissue necrosis was observed in any study. Interestingly, studies reported the presence of Fe laden macrophages ranging in localization from sparse isolated cells to clusters at the implant interface, which were present at time points from 1 to 33 months [100-103]. The solubility of Fe-bearing degradation products is very low in saline solutions, making it difficult for the body to clear them from the implant site [104, 105]. Indeed, the early studies report a pronounced accumulation of corrosion products at the implant site, with adjacent tissue staining positive for Fe residues. As a result, macrophages carry a heavy load in the clearance of ferric and ferrous Fe from the corroding implant, as evident by the Fe containing macrophages at the implant interface [104]. Peuster et al reported the clearance of Fe away from the implant starting at 1 month, as small amounts of Fe-containing macrophages were observed in the para-aortic lymph nodes. The amount of Fe laden macrophages in the para-aortic lymph nodes slightly increased with the corrosion of the implant at 3 months and continued to be observed for the duration of the 12 month study. However, histopathological examination showed no signs of Fe overload/toxicity in the para-aortic lymph nodes or heart, liver, spleen, lung and kidney tissue [101]. This suggests that a moderate level of chronic inflammation will be present and may be required for the lifetime of an Fe-based stent.

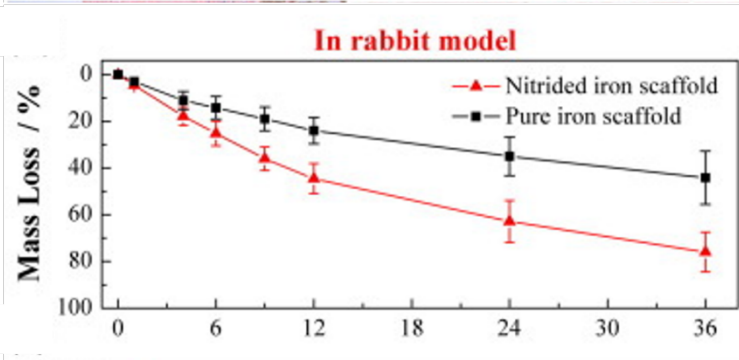
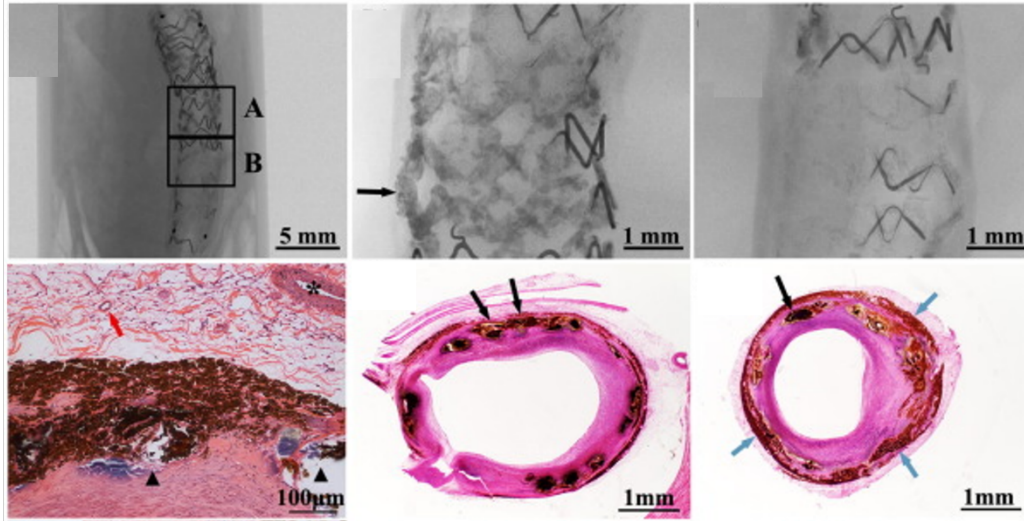
#### 4.1.2 Current status and future prospects of Fe stent development

The greatest recognized challenge in the field of Fe based BRS is developing processing techniques and alloyed compositions to increase the corrosion rate. If the stent remains in its host artery for an extended period of time before resorbing, the anticipated benefits of BRS such as the mitigation of late thrombosis and chronic inflammation or the resumption of physiological vasomotion are overshadowed by complications associated with the long-term presence of the implant. The development of nitrided Fe stents gained interest over the past decade due to their increased corrosion rate and mechanical properties relative to pure Fe stents [103, 104, 106-108]. The exceptional mechanical properties of nitrided Fe allow for stents with strut diameters of 70  $\mu\text{m}$ . Studies have fabricated nitrided Fe stents and implanted them into pig or rabbit arteries for an in vivo evaluation, as seen in Table 4. The biological response to the nitrided Fe stents was very similar to the first pure Fe implants (as shown in Fig. 4a). No thrombosis was observed in any of the studies. Moderate degrees of inflammation were observed along with relatively thin neointimal formations comprised primarily of SMCs. Chao et al reported no significant differences in neointimal thickness or area between the nitrided Fe stents and industry standard CoCr stent controls [106]. A pronounced amount of corrosion

**Table 4.** Summary of Fe based BRS studies. SEM: scanning electron microscopy, OCT: optical coherence tomography, NA: neointimal area

Ref	Stent	Endothelialization	Histological presentation	Inflammation
[100]	Pure Fe	Histology + SEM demonstrated a confluent endothelium	Thin neointimal formation composed of SMCs after 18 months of implant residency.	Moderate inflammation can be observed from histology. Macrophages appeared to contain Fe corrosion products.
[101]	Pure Fe	Histology revealed partial endothelialization by 2 weeks and complete endothelialization by 4 weeks	NA increased over time for both materials. The neointimas for both materials appeared very organized and comprised of SMCs	For 316L and Fe, at 1 day, neutrophils were found infiltrating the media next to the stent struts for both materials. Mild inflammation was seen surrounding the Fe stents starting at 2 weeks. Accumulation of iron laden macrophages within the media and adventitia is reported throughout the duration of the implantation
[102]	Pure Fe	No difference between Fe stents and contemporary permanent controls	Histology revealed slighter smaller neointimal thickness and area for the Fe group, no statistical significance	There were no statistical differences in injury or inflammation scores between CoCr alloy controls and the Fe stents
[104]	Nitrided Fe	SEM imaging showed a confluent endothelium at 1 month. Endothelialization was complete by 3 months.	Intimal thickness remained constant from 3 to 6 months, but significantly increased at 12 months	At 3 months, inflammatory cells could be observed adjacent to the stent strut. By 6 months, implant corrosion became more obvious and the inflammatory cells were still present. The inflammatory score at 12 months was significantly less than 3 and 6 months.
[106]	Nitrided Fe	Although the nitrided Fe stents were trending upwards, the % endothelial coverage was not significantly higher (84.38±14.50% vs. 65.00±22.04%, P=0.057) than CoCr controls	Mild to moderate hyperplasia was observed in 6 out of the 8 samples for each group. Severe neointimal hyperplasia was observed in two stents per group	No tissue necrosis was observed. Immunostaining for macrophages revealed no significant difference in the inflammatory response, where most stents in both groups had no MAC+ cells.
[107]	Nitrided Fe	OCT imaging revealed a thin and complete neointimal coverage of the stents by 3 months. Histology demonstrated complete endothelialization by 3 months.	Relatively thin neointimal formations from 3 to 13 months.	No signs of tissue necrosis were observed. They report a slight consistent inflammatory response up to 13 months after implantation.
[103]	Nitrided Fe	SEM demonstrated complete endothelialization of the nitrided Fe stent and only partial endothelialization for the 316L control at 7 days (rabbit model).	Very thin neointimal formations at 1, 6, and 12 months Thicker neointimal formations at 33 and 53 months are seen, suggesting a moderate degree of neointimal hyperplasia	Histology showed slight inflammation elicited by both materials at 1, 6, and 12 months. Macrophages engulfing corrosion products were observed at 12 months adjacent to the nitrided Fe stent.
[108]	Fe	By 28 days, endothelialization was the same and essentially complete for both materials. (77 ± 15% vs 30 ± 30% at 7 days (p = 0.032), 87 ± 8% vs 64 ± 17% at 14 days (p = 0.017), and 96 ± 3% vs 97 ± 2% at 28 days (p = 0.86) ) (% coverage of Fe stent vs industry standard DES)	OCT revealed no significant differences in intimal thickness between the Fe and industry standard DES and 28 and 90 days.	Histology demonstrated a consistent slight inflammatory response for both materials at 28, 90, and 180 days. Both injury and inflammation scores showed a decreasing trend over time for the Fe stent. The inflammatory scores for the Fe stents were trending in the higher direction than the industry standard DES at 28 and 90 days.
[109]	IBS	Complete endothelialization by 3 months	At 90 days, the IBS scaffold and Supporter (control) appeared to present similar histological findings	Phagocytosing macrophages present, but not yet presented to the lymph node, correlating with corrosion being in its earlier phases.

A.



B.

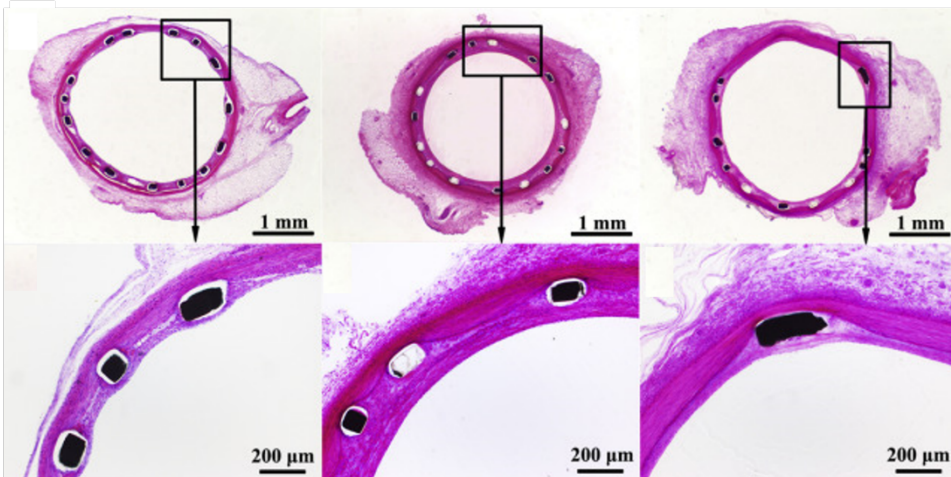
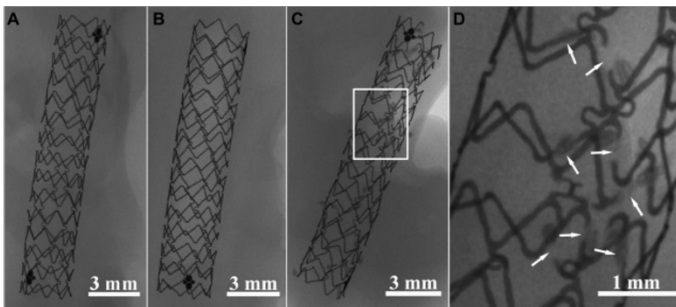


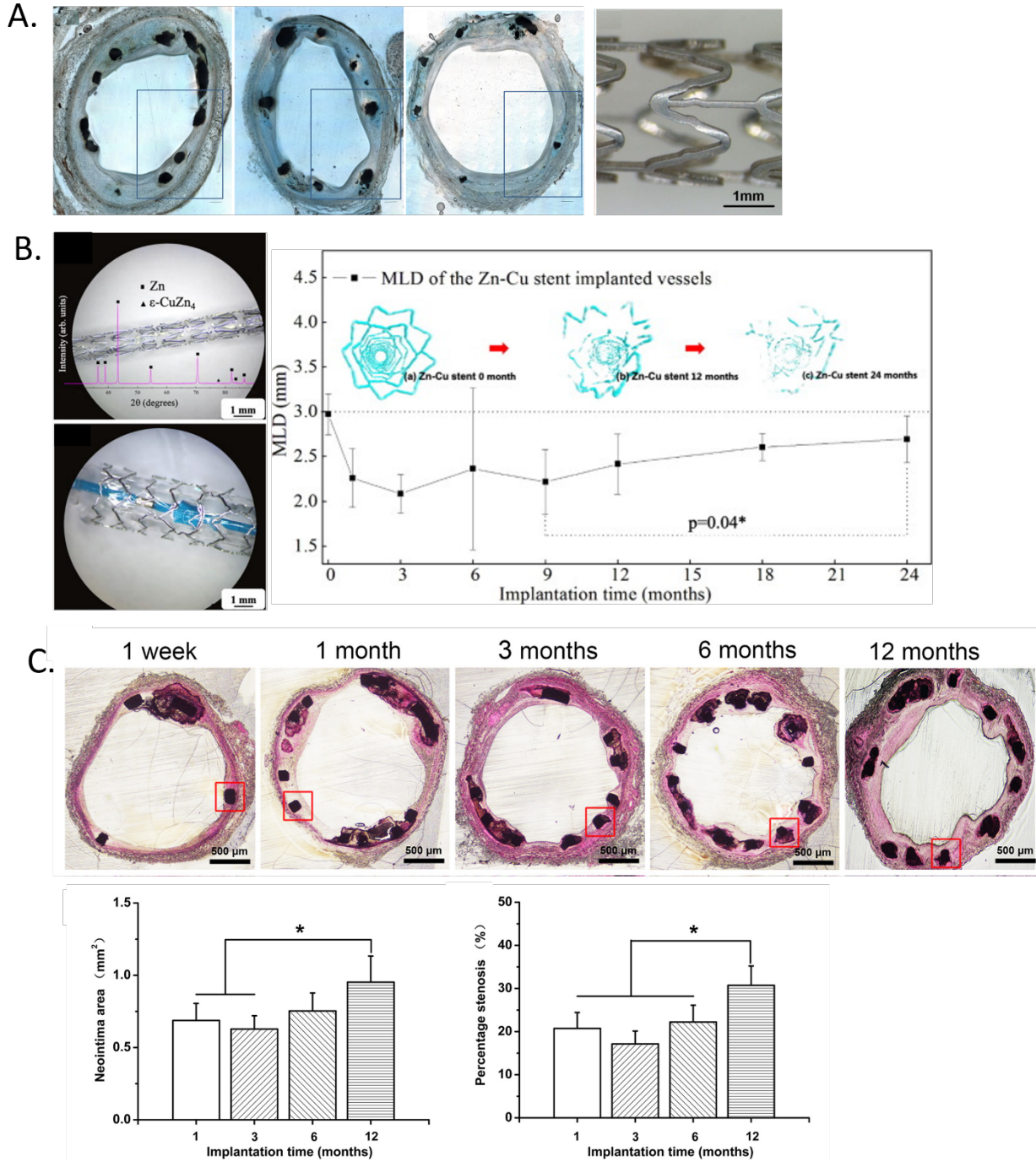
**Figure. 4.** Recent Fe-based scaffolds. a) Study from reference [103] outlines degradation of a nitrided Fe scaffold shown by micro CT 2-D images after 53 months in porcine coronary artery. Histology of the explant shows accumulation of corrosion product within the arterial wall. b) Recent preclinical success of IBS Fe stent implanted in porcine coronary arteries. First panel depicts the micro CT images of the sirolimus eluting IBS scaffold at 28, 90, and 180 days post implantation. The enlarged area shows local corrosion on the struts. The second row displays H&E stains of the IBS scaffold at 28, 90, and 180 days implantation. Adapted with permission from reference [108]

products were retained at the implant site. Additionally, endothelialization appeared to be complete by 1 month [104, 108]. Zheng et al reported a confluent eNOS+ endothelium at 1 month, demonstrating endothelial functionality [108]. In 2 cases, the nitrided Fe stents actually exhibited significantly higher rates of endothelialization relative to permanent industry standard controls, which is likely due to their reduced strut size [103, 108]. Lin et al implanted 70  $\mu\text{m}$  diameter nitrided Fe stents into porcine coronary arteries for up to 53 months [103]. They found that after 53 months of corrosion, there were no abnormalities in heart, liver, spleen, lung, or kidney tissue, suggesting that the corrosion products did not elicit toxic systemic effects. However, according to their in vivo corrosion rate analysis in a rabbit model, their nitrided Fe stents would require approximately 4-5 years to completely dissolve (Fig. 4a). Strategies to increase the corrosion rate include adding a polymer to the surface, for instance using degradable polyesters (PLA). These approaches have been moderately successful, with apparent acceptable in vivo biocompatibility, although the lack of data regarding in vivo endothelialization for these surface modifications make it difficult to draw definitive conclusions [110-112].

While it has become well accepted that Fe stents avoid systemic side effects, the local biocompatibility of Fe materials has recently come into question [113]. Scarcello et al showed that vascular cells in direct contact with Fe can incur substantial toxicity from the production of hydroxyl radicals during corrosion [114, 115]. In addition to the reduced cytocompatibility seen in the direct contact of vascular cells with Fe, the  $\text{Mn}^{2+}$  rich soluble corrosion products of Mn-alloyed Fe stent materials are particularly toxic to vascular cell types [116]. When taken together, attempting to increase the degradation rate of Fe could result in more intense inflammatory reactions than what has been previously seen for Fe. Although increasing the corrosion rate can be of particular concern in terms of byproduct exposure, the enhanced mechanical strength of Fe allows for thinner struts in the final stent, which could translate to fewer harmful corrosion byproducts and an increased absorption rate [107]. In summary, the local biocompatibility of Fe-based devices needs to be carefully investigated with proper material controls. Additionally, thorough assessment of stented lesion outcomes after full degradation of the device still need to be reported [19]. While the local effects of Fe corrosion on neighboring tissue and cells are beginning to become clearer, the preclinical success (shown in Figure 4) of the IBS scaffold demonstrates the promising potential of Fe-based stents [108, 109, 117].

## 4.2 Zn based materials

### 4.2.1 Early in vivo examination



Zn based materials have emerged as promising BRS candidates due to more favorable in vivo corrosion rates relative to Mg and Fe, and suitable mechanical properties when alloyed [15, 121]. In 2017, Yang et al. were the first to implant 24 pure Zn stents (165  $\mu\text{m}$  strut thickness) into the abdominal aorta of rabbits and evaluate the biological response from 3 days up to a year [122]. After 3 days, no significant platelet adhesion or membranous thrombus formations were observed. By angiography, no arteries lost complete patency for the duration of the experiment. Immunohistochemistry for CD31 revealed a confluent endothelium by 1 month. The thickness of the neointima also appeared to slowly increase over time, but no major neointimal hyperplasia was observed. Indeed, angiography revealed a slow increase in mean diameter stenosis over time. However, the mean diameter stenosis was substantially less than 10% at 12 months. Immunostaining for macrophages revealed the highest level of inflammation at 1 month, which slowly decreased for the duration of the experiment, with most macrophages localized near the stent strut. In one case, a complete local degradation of a stent strut was observed at 12 months. However, no obvious accumulation of corrosion products was observed throughout the study. Although pure Zn has insufficient mechanical strength to effectively serve as a scaffold in an atherosclerotic lesion, this was a landmark proof of concept study in demonstrating the exceptional in vivo corrosion characteristics and suitable biocompatibility of Zn. As a result, materials scientists have been highly motivated to develop Zn based materials, primarily through alloying, with increased mechanical strength.

#### 4.2.2 Current status and future prospects of Zn stent development

The current challenge in the Zn based BRS field lies in developing materials with suitable strength for vascular stenting applications without sacrificing the in vivo corrosion characteristics and biocompatibility that make Zn such a promising BRS candidate material. Since Zn's introduction to the BRS field in 2013 [123], there have been many efforts to optimize Zn's material characteristics for stenting properties, primarily through alloying [15]. To the authors knowledge, there have been four studies where Zn alloy stents have been fabricated and implanted in animal models.

In 2018, Lin et al implanted 20 Zn-0.02 Mg-0.02 Cu (wt%) stents in the left carotid artery of New Zealand white rabbits [120]. Stents were evaluated for endothelialization (by en face imaging), corrosion behavior (by micro-CT), and histology at time points ranging from 1 week to 12 months. The stents displayed a highly localized corrosion mode with partial strut corrosion seen at 12 months, which had also been seen at 12 months for pure Zn stents [122]. Endothelialization of the stents at were complete by 1 week, as rabbits typically exhibit faster endothelialization rates relative to porcine models. The neointima area gradually increased over time (Fig. 5C), with the lumen stenosis around 30% at 12 months.

In 2019, Zhou et al implanted 40 Zn-0.8Cu (wt%, 100  $\mu\text{m}$  strut thickness) stents into the coronary arteries of female Shanghai white pigs and evaluated the biological response at time points ranging from 1 to 24 months [119]. They reported a similar biological response to the pure Zn study, with endothelialization being complete by 1 month. Macrophages were observed at the implant interface at 3 months, and the degree of inflammation appeared to slowly decrease at 9 months. Interestingly, by angiography the minimum lumen diameter significantly improved from 9 to 24 months (Fig. 5b), suggesting positive remodeling with the degradation of the stent.

Hehrlein et al. fabricated Zn-3 wt% Ag stents and implanted them in 15 juvenile domestic swine for 1, 3 and 6 month time points (n=15 iliofemoral artery stented segments) [118]. Angiography showed successful stent deployment, with minimal luminal narrowing at the 1, 3, and 6 month follow up times. Evidence of scaffold degradation can be seen in histological cross-sections taken at each time point, in Fig.

5a, although the direct in vivo biocorrosion rate was not measured. The same research team followed up development of Zn-Ag stents with fabrication of an “ultrathin strut” design to help alleviate stent jailing in bifurcated lesions. The combination of thinner struts and the addition of a sirolimus releasing coating significantly reduced neointimal formation ( $14.5 \pm 1.1$  vs  $9.9 \pm 0.5$  vs  $8.7 \pm 1.2$  mm<sup>2</sup>, large strut vs thin strut vs thin strut+ drug eluting coating, respectively), further demonstrating the efficacy of Zn alloy based stents [124].

In summary, Zn based stent studies revealed no cases of scaffold thrombosis and similar endothelialization properties to Fe and Mg stents in preclinical models. Promising degrees of SMC neointimal hyperplasia and inflammation were also observed. Scaffold degradation appears to suffer from localized corrosion, which may be improved by thermomechanical processing. Overall, the results suggest great biocompatibility for zinc based BRS. At this time, the field would benefit from stent implantation studies comparing the performance of Zn based BRS to industry standard BMS and DES controls. Although the field continues to actively and productively develop Zn based materials with improved strength [125], our understanding over how material modifications effect in vivo corrosion behavior and biocompatibility has not kept pace. Improving our understanding of these relationships will allow us to develop materials with not only improved mechanical properties but improved clinical outcomes.

## 5. Understanding the relationship between material characteristics and the neointimal response

As highlighted throughout this review, proper mechanical properties of stent materials are critical for clinical success. Insufficient mechanical strength can limit stenting applications to short, non-calcified lesions, as seen in the case of Mg based BRSs. On the contrary, exceptional mechanical strength can allow for ultra-thin strut design, leading to improved hemodynamics, and ultimately improving the biological response. As a result, most studies in the BRS field focus primarily on improving mechanical properties. Although improving mechanical properties is vital for the advancement of the BRS field, there is a major gap in our understanding between material characteristics and the neointimal response of implanted degradable materials. Modifications, such as alloying, surface treatments, and manufacturing/processing techniques all affect corrosion characteristics. Changes in the rate of corrosion, dissolution mechanism, localization/uniformity, and by-products will all affect how the local tissue responds. Improving our understanding over the relationship between material characteristics and the resulting biological response will allow us to engineer materials with improved clinical performance. In this section, we aim to review studies which highlight the relationship between material characteristics and the resulting neointimal response. Significant advances in the clarification of neointimal responses for Zn based materials has been conducted by our group, and this class of materials will comprise a majority of those covered in this section.

### 5.1 Development of the rodent wire implant model

While in vitro models are an efficient approach to prescreen the biocompatibility of novel BRS materials, they are a gross oversimplification of the applicational arterial space. Blood and protein/material interactions, pulsatile flow, vasomotion, and eventually complex cell/material interactions all contribute to the corrosion behavior of a BRS material. Additionally, the complexity of signaling between the initial

coagulation cascade and the ensuing cellular response, which involves cross talk between the endothelium, SMCs, and both circulating and tissue residing inflammatory cells, cannot be replicated in vitro [126]. Therefore, in order to comprehensively study the relationship between material characteristics, corrosion behavior, and the neointimal response, in vivo models which examine BRS materials in the arterial space must be utilized. In 2012, Pierson et al. proposed a wire implantation model wherein candidate metallic stent materials drawn to wires are implanted into the abdominal aorta of adult Sprague Dawley rats to simulate a stent strut, as depicted in Fig. 6a [105]. The major advantage of this model is that it allows for an efficient in vivo analysis of absorbable stent candidates relative to the high cost, specialized equipment, and clinical expertise required to fabricate and implant stents in large animal models. Additionally, the rodent model allows for comprehensive histological evaluation at the implant interface with the host artery, and high sample size analyses can be leveraged to relate material properties and their resulting corrosion behavior to the ensuing biological response. Because the murine preclinical model makes use of a single wire implant to simulate the presence of a stent strut within the vascular space, the extensive endothelial denudation and vessel injury associated with delivery of stents is eliminated. This allows for relating the biological response to the behavior of the material of interest, without the confounding variables associated with stent design, mechanical properties, and implantation injury. Guillory et al recently developed a quantitative neointimal morphometric approach for evaluating the biocompatibility of absorbable materials using this animal model [127]. Neointima tissue surrounding the wire implant was measured for area, thickness, and protrusion into the arterial lumen. Neointimal morphometrics - wire lumen thickness (WLT), neointimal area (NA), and base neointimal length (BNL) depicted in Fig. 6 b<sub>1</sub> were proposed as metrics to assess biocompatibility in stenting applications. Based on these metrics, the lumen occlusion index (LOI) was calculated, as explained in Fig. 6b<sub>1</sub>, as a corollary to the diameter stenosis metric commonly used to assess stents clinically. Guillory et al. suggest that LOI values greater than 30% or WLT values greater than 70 μm define implant failure. Table 5 summarizes studies performed that utilize the murine-based wire implant model to understand the neointimal response to the corrosion of candidate BRS materials.

## 5.2 Effects of BRS material class on neointimal response

In the first report to utilize the wire implantation model, Pierson et al. implanted pure Fe and Mg wires for time points of 22 days, 1.5, 3, 4.5, and 9 months [105]. Corroborating with previous reports of stent implants in larger animal models, the Fe wires corroded at a slower rate and retained a pronounced amount of corrosion products at the implant site relative to their Mg counterparts. This once again highlights the difficulty of Fe corrosion product removal by local cells. Interestingly, the study revealed that for both the Fe and Mg wires, the corrosion rate was notably higher on the wires implanted in the arterial wall as opposed to the lumen. This demonstrates the importance of developing blood contacting in vivo models to evaluate the corrosion behavior of BRS materials. In 2015, Bowen et al. made use of the wire model to showcase the difference in corrosion rates of pure Mg wires in the arterial wall compared to in vitro experiments in simulated body fluid (Dulbecco's modified eagle medium) [128]. These findings highlight the importance of using in vivo models to evaluate corrosion kinetics, as they more closely replicate the corrosion behavior of a full BRS in larger animal study or in the clinic.

Much of the pioneering work in the Zn based BRS field was done utilizing the wire implant model. Early studies demonstrated that Zn is well tolerated within the rat abdominal aorta. In contrast to corrosion

resistant metals that display a rigid and impenetrable interface to inflammatory cells, it was shown that Zn materials develop a dynamic interface that permits the penetration of inflammatory cells, phagocytic activity, and biomatrix regeneration. The degradation rate of Zn materials is also found to be within the desired range of 0.02–0.03 mm/year. Additionally, local tissue response to the Zn implants revealed evidence of early tissue regeneration around the biocorrosion area, with no sign of local or systemic toxicity. It was shown that Zn implants could remain intact for the first 3–4 months of implantation due to the formation of a protective oxide film on the implant surface. After a few months in vivo, the corrosion products were primarily benign compacted Zn oxides and Zn carbonate. Histology and immunostaining revealed relatively small neointimal formations comprised of a thin layer of SMCs, a moderate to low level of inflammation at the implant interface, and a confluent endothelium at the earliest investigated time point of 2.5 months [129]. These findings were corroborated by Yang et al upon implantation of pure Zn stents into the abdominal aorta of rabbits two years later [122].

In 2020, Fu et al utilized the wire model to demonstrate the in vivo corrosion behavior of pure Zn and the Mg alloy WE43 relative to inert 316L stainless steel controls and the biological response to the corrosion was examined [11]. Histology and immunostaining for CD11b demonstrated that the Mg implants elicited a minimum inflammatory response, which was resolved by 24 weeks, whereas Zn and 316L implants elicited higher degrees of inflammation. Staining with picosirius red demonstrated neointimal formations surrounding the Mg implants were more densely packed with collagen fibers than the Zn and 316L implants. Qualitatively, the presented histology figures demonstrate that at the early time point the Mg wire elicited the thickest neointimal formation. These findings suggest that for Mg, inflammation is not the major driver of neointimal formation, but rather SMC neointimal hyperplasia. On the contrary, Zn corrosion appears to elicit higher degrees of inflammation relative to Mg. These findings corroborate with recent work done by our MTU group that has suggested that inflammation is the major factor contributing to neointimal formation in Zn based materials [130]. This work highlights how use of this wire model to observe the effects of material characteristics on the biological response can inform the design of improved stent materials. In this case, it demonstrates how Mg based BRS materials may require a drug eluting coating to mitigate neointimal hyperplasia, while Zn based BRS materials must be designed with the priority of minimizing the inflammatory response.

### 5.3 Effects of surface treatment on neointimal response

Surface modification techniques can be used to modify the short-term corrosion behavior of BRS materials. Therefore, utilization of these techniques is a great opportunity to modulate corrosion behavior in order to fine tune the biological response. Guillory et al. utilized the wire implant model to investigate how engineered surface oxide layers on pure Zn wires affect the corrosion rate and the resulting biological response [131]. Pure Zn wires were either electropolished or anodized to produce distinctive physical and corrosion characteristics. In vitro corrosion analysis revealed that the anodic coating improved corrosion resistance and led to uniform surface dissolution, in contrast to the localized pitting observed on electropolished surfaces. Moderate, more homogenous corrosion of the anodized implants improved the biocompatibility in terms of neointimal morphometrics relative to the localized variable pitting corrosion behavior exhibited by the electropolished implants. Therefore, this data suggests that surface treatments which increase the uniformity of corrosion, and minimize pitting behavior, will improve the biological response.

### 5.4 Effects of alloying on neointimal response

While alloying is a commonly used, effective method of improving the mechanical strength of BRS materials, careful consideration must be made when making elemental additions. Although alloying may drastically improve mechanical properties, it can also affect the neointimal response. In vivo studies utilizing the wire implant model have revealed marked differences in inflammatory response, attributed to the compositional dissimilarities of alloys that cause variations in implant corrosion behavior. Wires made of pure Zn, Zn-Al, Zn-Mg, Zn-Li, and Zn-Ag alloys were implanted into rat artery lumens to investigate biological responses of arterial environments to metals [127, 130, 132, 133]. In addition, the performance of Zn after different surface treatments have been analyzed. In general, the addition of alloying elements reduced the biocompatibility of Zn-based materials. Zn-Al alloys exhibited an intergranular corrosion vs. the surface corrosion that has been observed for pure Zn and other Zn alloys investigated so far [134]. Qualitative histological analysis revealed higher degrees of inflammation elicited by the Zn-Li and Zn-Mg implants and possible impaired endothelialization elicited by the Zn-Mg alloys [45, 132, 133]. A decrease in biocompatibility as a result of alloying Zn is a common trend, however the reason still remains unclear. Figure 6 demonstrates a decrease in biocompatibility for Zn-Li, Zn-Mg, and Zn-Ag alloys relative to pure Zn. It was speculated that  $Mg_2Zn_{11}$  particles promote a more aggressive activity of macrophages in an attempt to metabolize this alloy phase known for increased corrosion resistance, although this remains to be proven. Similarly, the greater inflammatory response exhibited by Zn-Li implant was attributed by the increased variety of chemical species displayed to immune cells during the course of dissolution process, such as the  $LiZn_4$  intermetallic. An enrichment of intermetallic particles in the corrosion product layer during in vivo degradation of Zn alloys and their effect on tissue regeneration is of concern and has not been addressed yet.

In the most recent contribution from our group, the biocompatibility of Zn-Ag-based systems were investigated (Table 5) [130]. Zn-4Ag, Zn-4Ag-0.6Mn, and Zn-4Ag-0.6Mn-0.15Zr-0.6Cu wires, as well as pure Zn and Pt control wires were implanted into the rat abdominal aorta for 6 months. A comprehensive evaluation of the inflammatory profiles using immunofluorescence techniques demonstrated a notably worsened arterial inflammatory response elicited by the Zn-4Ag and Zn-4Ag-0.6Mn alloys. Surprisingly, the Zn-4Ag-0.6Mn-0.15Zr-0.8Cu alloy elicited an inflammatory response similar to that of pure Pt controls and most notably a more favorable inflammatory response than the pure Zn control (as illustrated in Fig. 6c). This study demonstrated that elemental additions to materials (Zr and Cu in this case) can result in changes to the in vivo corrosion behavior and composition of corrosion products that ultimately improve the biocompatibility. More work needs to be done to clarify the exact mechanisms by which particular alloying additions result in favorable biological outcomes.

### 5.5 Effects of corrosion byproducts on neointimal response

The wire implantation model has also been used to investigate the effects of corrosion products on the surrounding tissue. In the first comprehensive evaluation of the biological response to Zn corrosion in the arterial environment, Bowen et al. reported that  $\alpha$ -SMA immunostaining revealed a distinct lack of VSMCs adjacent to the implant [129]. Bowen speculated that corrosion products from the corroding Zn wire may elicit an antiproliferative effect on VSMCs, as this effect is not typically seen for BMS or other BRS materials. These findings were later corroborated by Yang et al, after implantation of pure Zn stents into the abdominal aorta of rabbits [122]. Since SMC hyperplasia is the primary cause of stent failure in the clinic, our group decided to investigate this phenomenon more thoroughly. To this end, pure Zn and Pt (bioinert permanent control material) wires were implanted into the rat abdominal aorta. Immunostaining revealed a reduced amount of  $\alpha$ -SMA + cells in the neointimal formations elicited by the

pure Zn wires as opposed to Pt [135]. The pure Zn neointimas also possessed a significantly higher amount of TUNEL and active caspase-3 signal, indicative of a VSMC suppressive effect via caspase 3 dependent apoptosis. VSMC neointimal suppression adjacent to Zn implants is shown in Figure 7, which also demonstrates the persistence of this phenomenon across multiple animal models and Zn based materials. Similar to DES, the elution of  $Zn^{2+}$  from the material as it corrodes could act as a therapy that prevents the proliferation of SMCs and tissue protrusion into the lumen. The data from these studies showed that  $Zn^{2+}$  could specifically targets VSMCs, as endothelial cells completely regenerated over the neointimas of Zn-based arterial implants in a number of studies from different groups. This effect stands in contrast to drug eluting stents, where antiproliferative effects target all local cells non-specifically. Another benefit of Zn-based materials over those that require drug eluting polymer coatings is that  $Zn^{2+}$  will continue to elute and provide anti-SMC therapy for the lifetime of the implant. These are both advantages over conventional DES, whose drugs target SMCs amongst other non-specific targets, resulting in potentially negative side-effects including delayed endothelialization.

#### 5.6 Effects of microstructure and manufacturing processes on neointimal response

In addition to the chemical composition, microstructure also plays a key role in the biocompatibility of biodegradable metals. Microstructure impacts the biomechanical compatibility and ion release profile of biodegradable stents. Metallic stents are manufactured by either wire braiding or tube laser cutting. In both cases the stent material undergoes massive cold metal working. Unfortunately, the effect of cold working on mechanical performance and biomechanical compatibility has been largely neglected in the literature. Besides mechanical properties improvement, the microstructure design of Zn alloys helps to avoid any biomechanical damage caused by localized corrosion. A recent contribution by Mostaed et. al proved that cold working considerably changes the mechanical and corrosion performance of Zn alloys [136]. Indeed, Zn alloys after cold working experience significant drop in mechanical strength as well as distinct deterioration of the corrosion resistance. Accordingly, the microstructure design of Zn alloys helps to avoid any loss of strength and corrosion induced-mechanical degradation. Laser cutting can generate local microstructural changes due to the thermal processes [137]. Such heat effect can be limited depending on the employed laser type, while the ultrafast laser sources appear to be the solution for Mg and Zn alloys due to their higher sensitivity to heat [138]. Chemical and electrochemical finishing processes are often employed to remove the dross and heat affected zones after laser cutting. However, the control of the material removal extent by these processes is difficult due to the intrinsic degradation behavior of these alloys [139, 140]. Within the manufacturing chain an annealing stage may be required to retain the desired properties after laser cutting. In brief, the selection of materials for absorbable Zn-based stents should not be based on the mechanical, corrosion, and biocompatibility testing on thermomechanically-processed parts (as-extruded, as-rolled etc.) as they dramatically differ from those of the final stent products, which are subjected to an entire manufacturing chain including cold drawing often followed by thermal cutting and finishing operations [16]. From this perspective, the manufacturing fingerprint should be better represented at the material development stage for more reliable models. The wire implant model provides a reasonable step forward also from this perspective.

Surface modification techniques can significantly alter short-term and long-term in vivo performance of cardiovascular implants as well provide them with certain biological functions, while the main goal of the alloying and microstructure design of Zn-based stent materials is the improvement of mechanical properties, and reduction of corrosion damage by augmenting degradation uniformity and mechanical integrity of the alloys. The elements with the potential toxicological problems must be avoided or used in

the concentration that is not toxic to the host, while designing the novel cardiovascular Zn-based alloys. Similarly, the degradation products should be non-toxic and easily absorbable by surrounding tissues. Certain ions released during the progressive in vivo dissolution of Zn alloy (for example Zn, Cu or Zr) can enhance the implant biocompatibility in the arterial environment. The controlled release of these elements can be realized by proper microstructural design and/or surface treatments.

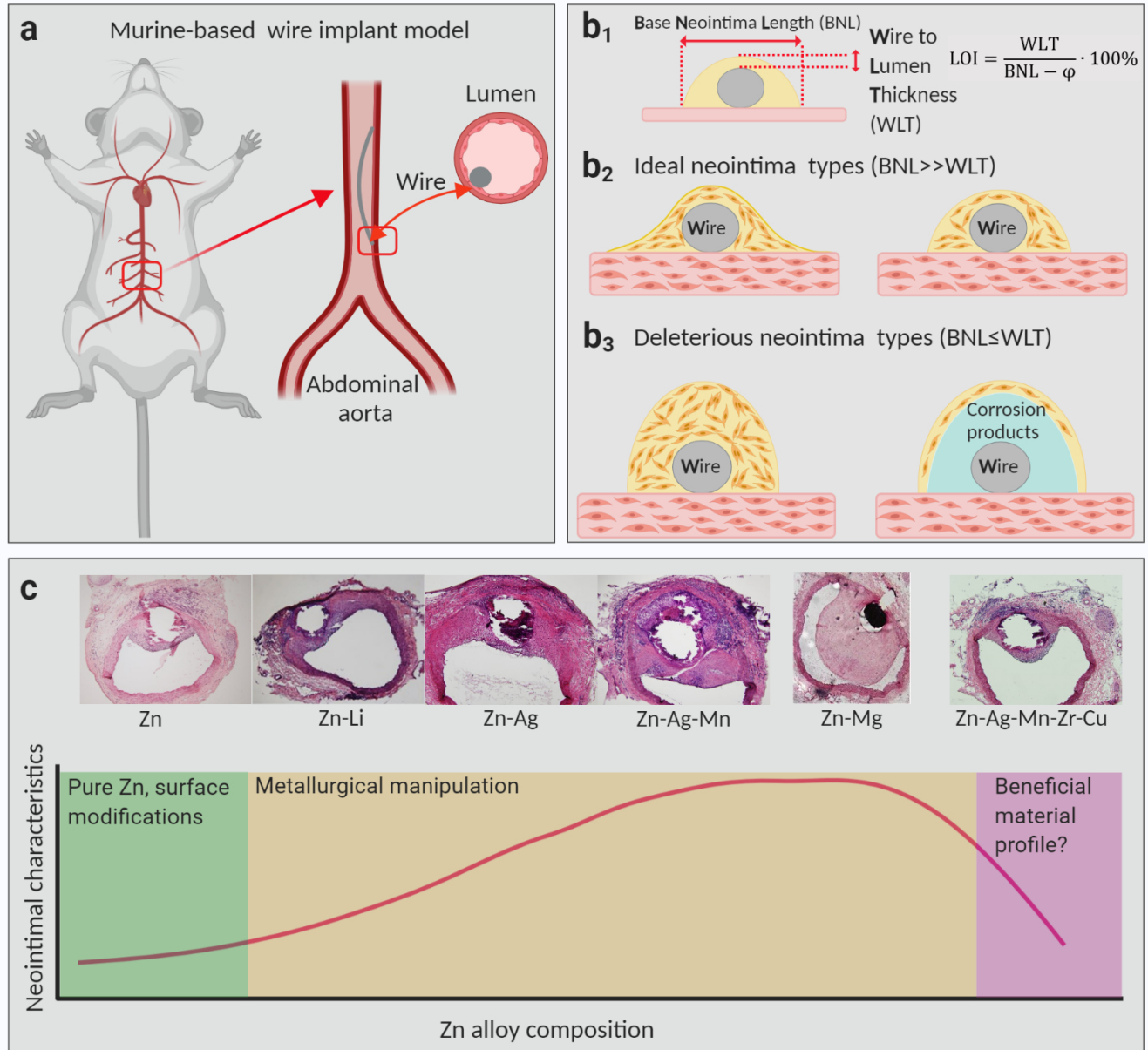


**Figure 6.** (a) Murine-based wire implant model, (b<sub>1</sub>) scheme of neointimal morphometrics with measurement locations in relation to the neointimal formation, and various neointima types dominating in most observations in wire model: (b<sub>2</sub>) Ideal neointima types with a low profile and stable mature tissue response, and (b<sub>3</sub>) negative neointimal responses contributing to luminal area reduction and reduced vascularization, and voluminous corrosion products formation, (c) H&E staining of different Zn-based explants after 6 months of implantation showing ideal or deleterious neointimal formations as a function of the implant elemental composition. H&E staining adapted with a permission from references [130] (Zn and Zn-Ag-based wires), [133] (Zn-Li wire), and [127] (Zn-Mg wire) Created with BioRender.com

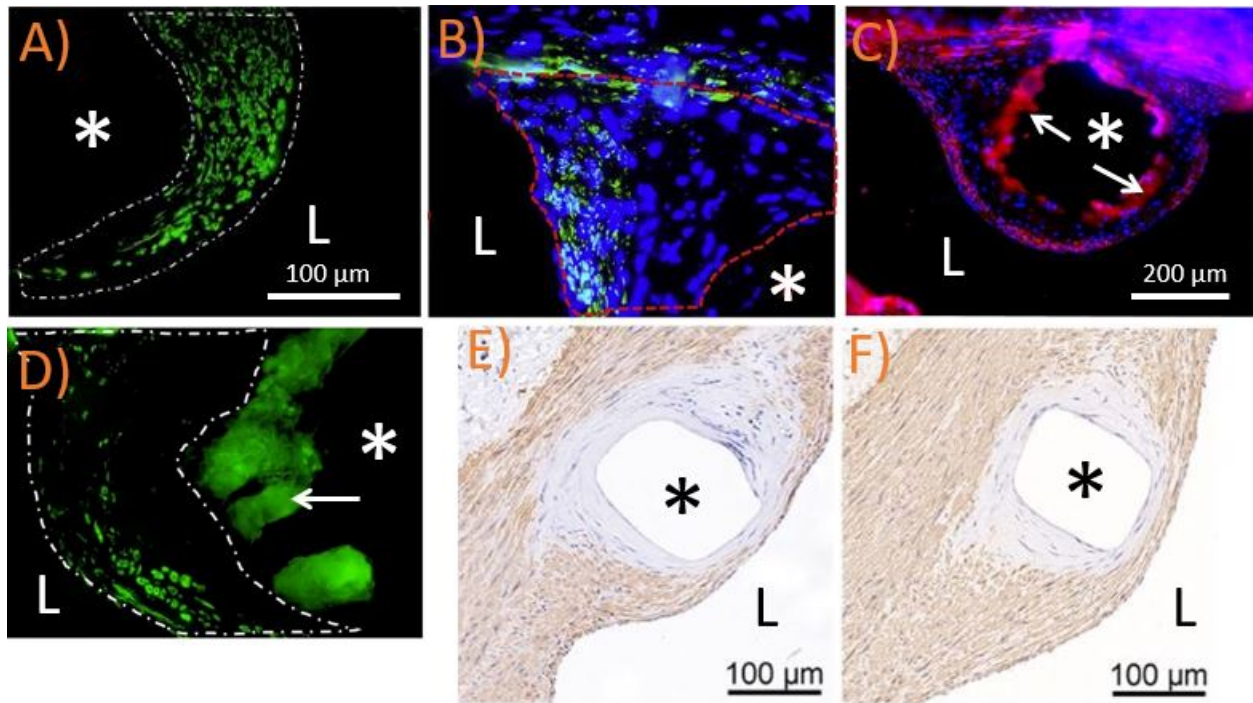


**Figure 7.** A) Pt implant (\*) at 6 months in rat wire model demonstrating typical ASMA+ cell (green signal) localization in neointimal formations (outlined by dashed line) to biostable stent materials (60X) [130]. B) Representative neointimal ASMA+ cell localization to pure Zn implants in rat wire model (3-month implant residency, 60X) [135]. C) low magnification image (20X) of representative ASMA+ cell localization (red signal, highlighted by white arrow) to pure Zn implants after 6 months of implant residency in rat wire model [129]. D) Representative neointimal ASMA+ cell (green signal) localization to Zn alloy implants (ZnAgMn in this case) after 6 months of implant residency in rat wire model [130]. E & F) IHC for ASMA (brown signal) at 6 and 12 months respectively for pure Zn stents in the rabbit abdominal aorta [122]. "L" identifies the lumen and \* identifies the strut/wire location in each image. White arrows indicate auto fluorescing corrosion product, which is clearly distinguishable from positive  $\alpha$ -SMA signal.

Material		Implantation duration (months)	Major Findings	Ref.
BRS materials	Zn wire, 99.99% purity	1.5 3.0 4.5 6.0	<ul style="list-style-type: none"> <li>Penetration rate &amp; immediate effects of generated corrosion products fulfill the requirements for stent application</li> <li>Zn implant remained intact for 4.5 months</li> <li>Corrosion products consisted mainly of ZnO &amp; ZnCO<sub>3</sub>.</li> </ul>	[121]
	Zn wire, 99.99% purity	2.5 4.0 6.5	<ul style="list-style-type: none"> <li>Excellent biocompatibility with arterial tissues</li> <li>No inflammatory response</li> <li>No progressive intimal hyperplasia</li> </ul>	[129]
	Zn wires -99.99% purity	from 1 to 20 months	<ul style="list-style-type: none"> <li>Degradation progressed linearly for both cross-sectional area reduction (CSA) &amp; penetration rate, with up to 60% CSA reduction at 20 months</li> <li>Long-term implantation produced a thick corrosion layer &amp; fibrotic encapsulation of the implants</li> </ul>	[141]
	<ul style="list-style-type: none"> <li>Zn wire</li> <li>SS 316L</li> <li>WE43</li> </ul>	0.5 1.0 2.0 3.0 6.0	<ul style="list-style-type: none"> <li>WE43 wires showed the fastest degradation &amp; completely dissolved by 6 months</li> <li>Zn wires degraded 40% of their mass after 6 months</li> <li>SS wires degraded 10% of their initial mass over the whole experimental period</li> <li>Fibrotic encapsulation &amp; necrosis around wires persisted in Zn &amp; SS group</li> <li>WE43 showed normal morphologies of vascular walls</li> </ul>	[11]
	<ul style="list-style-type: none"> <li>Zn wires -99.99% purity</li> <li>Pt wire</li> </ul>	3.0 6.0	<ul style="list-style-type: none"> <li>Neointimal cells surrounding Zn implants were significantly more TUNEL positive &amp; alpha-actin negative than Pt controls</li> <li>CD68 &amp; iNOS markers were not increased in</li> </ul>	[135]

			neointimal tissue by Zn relative to Pt control wire ■Ionic Zn was confirmed to promote SMC death by activating the caspase-3 apoptotic signaling pathway	
Zn-based alloys	■Zn-Li ■Control: pure Zn	2.0 4.0 6.5 9.0 12.0	■Zn-Li retained ~70% of its original dimension after 12 months follow up; ■Zn-Li exhibited linear relationship between area reduction percent/implantation time ■Based on the histology Zn-Li alloys exhibited greater inflammatory reaction than pure Zn	[142]
	■Zn-xAl (x=1, 3, 5)	1.5 3.0 4.5 6.0	■No necrotic tissue, no indications of chronic or acute inflammation were observed ■Biocorrosion rates for Zn-Al were higher at initial stages as compared to pure Zn ■Zn-Al featured detrimental intergranular corrosion causing implant fragmentation	[143]
	■Zn-xMg (x=0.002; 0.005; 0.08)	1.5 3.0 4.5 6.0	■Zn-Mg alloys degraded uniformly ■Increase in degradation rates in later stages of implantation was observed ■Biocompatibility was reduced with increasing Mg content ■Corrosion resistant Mg <sub>2</sub> Zn <sub>11</sub> intermetallic phase causes a more aggressive macrophage activity	[144]
	■Zn-Ag ■Zn-4Ag-0.6Mn ■Zn-4Ag-0.6Mn-0.15Zr-0.6Cu ■Control: Pure Zn & Pt	3.0 6.0	■Cu-bearing alloy featured pronounced inflammation resistant properties relative to pure Zn ■SMC suppression near the implant interface observed in pure Zn & its alloys ■Inflammation degree against Zn-based implants is a greater contributor to neointimal growth than SMCs hyperplasia.	[130]
Surface treatments	Zn wires -99.99% purity: ■PLLA coated ■Control: pure Zn	0.5 3.0 4.5 6.0	■PLLA coating on MPS modified Zn wire reduced corrosion rate of the implant ■Histological analysis of arterial explants indicates detrimental effect of the PLLA on the biocompatibility of Zn ■Reduced cell biocompatibility with signs of toxicity & active neointima were seen after 3–6-month residency in the rat artery for PLLA coated wires	[145]
	Zn wires -99.99% purity: ■electropolished, ■oxidized ■anodized ■untreated Zn	1.0 2.0 3.0	■Zn corrosion rate varied with different surface engineering of thin oxide films degradation rate depended on the quality & stability of the oxide film ■Electropolished & anodized wires degraded slower than oxidized & untreated Zn in the rat artery	[146]
	Zn wires -99.99% purity: ■Electropolished pure Zn ■Anodized pure Zn	0.5 1.0 2.0	■Anodized wire revealed the highest corrosion resistance ■Anodized film acted as a barrier limiting the contact of the wire with physiological environment ■Histomorphometry revealed that electropolished wires elicited high variability with a high rate of failure ■In contrast, the anodized samples did not elicit any failures. ■Corrosion of electropolished wires was localized	[131]

**Table 5.** Summary on *in vivo* Zn-based wire studies using murine-based implantation model

## 6. Future directions

In the present review, we have summarized important current developments in metallic BRS technology. Mg remains the most studied bulk material for use as a BRS and has seen success in the clinic as discussed in section three of this review [55]. This success has been limited, as degradation rates for even the most advanced materials outpace arterial healing. This has translated to slightly inferior results relative to leading DES platforms [54]. Fe is the second most studied bulk material, but remains unproven in the clinic although preclinical studies involving the IBS scaffold with a sirolimus drug eluting coating appear promising [108]. Outstanding questions for this material include the nature of persistent inflammation and compatibility of its corrosion byproducts [113-115]. Data from an ongoing IBS scaffold clinical trial, which is expected to end in 2024, should shed light on the efficacy of Fe-based scaffolds (Lifetech

Scientific, 2018 start date). Zn remains the most undeveloped BRS bulk material, although preclinical studies demonstrate promising results for this class of scaffolds [118-120, 122, 124]. Our group has shown interesting relationships between neointimal growth and development and material properties for Zn-based materials [120, 127, 129, 131-135], although development of more advanced alloys to reach mechanical benchmarks are required [15, 80].

Recent efforts in Mg, Fe, and Zn based materials include elemental profile changes as well as surface modifications to improve flaws particular to each of the three classes of materials. Many reports focus on enhancement of particular beneficial biological processes by surface changes (such as reendothelialization), but the translation of these modifications remains limited. Mg stents in the clinic and the recent IBS scaffold both contain drug eluting coatings to help mitigate stent injury responses and intimal progression during the early lifetime of the implant. The inclusion of a drug releasing polymer would negate the effect of any surface modification to augment endothelialization, and presents a limitation of Fe and Mg-based stents [147]. Currently, the task force on clinical practice guidelines recommend DES for patients that present with comorbidities that increase the risk of long-term stent failure, such as diabetes [32, 33]. Additionally, any patient that receives DES therapies must undergo uninterrupted DAPT for at least 6 months (unless the patient expects to undergo additional surgeries within the year of stent placement, in which DAPT must be disrupted) [32]. The non-trivial expense of 12-month DAPT and additional complications that arise from the local and systemic effects of long-term drug elution prompts the selective use of DES, with a place for BMS still remaining in the clinic.

The development of a BRS without a polymer-based drug eluting coating, possessing adequate mechanical characteristics and a proper corrosion profile could thrust BRS into more widespread use in the interventional cardiology field. The biological effect of a degrading metallic material not only needs to be properly characterized, but also controlled. We have shown evidence that neointimal responses can be modulated with Zn based materials, depending upon the surface and bulk material components [127, 130, 131]. Investigations of Fe materials point towards a more inflammatory dominant reaction due to inherent properties of the Fe corrosion process, and this has yet to be studied in the detail that Zn materials have.

### 6.1 Models for in vivo evaluation of BRS materials

The current in vivo testing framework also has limitations. Rats, rabbits, and pigs, differ physiologically from humans. Positive outcomes observed in animal models do not translate directly to humans. Porcine models were unable to predict the limitations of polymeric resorbable scaffolds that eventually led to dramatic failure in clinic trials. Additionally, need for drug eluting coatings on bare metal stents was learned from experience gained from human studies [148]. The reliance on animal testing for vascular stents poses many challenges, largely stemming from differences in reendothelialization rates, blood chemistries and total cellular profiles, faster regeneration seen in animals, and lack of large phenotypic heterogeneity in lab strains of rodents, rabbits and pigs. Additionally, almost all animal testing occurs in healthy animals, while the ultimate application for a device such as a stent is typically subjected to a variety of arterial conditions with varying lesion characteristics in the context of progressive cardiovascular disease [149].

Simulating realistic physiologic conditions is critical when evaluating materials for human use. Early in vitro testing of materials was largely performed in crude simulated salt solutions. Exploring material degradation and interfacial interactions in protein and cell containing solutions has recently gained more attention [150-154]. Clarifying the influence of cells and proteins on the degradation of biodegradable

metals is essential for understanding and predicting the behavior of Mg, Fe, and Zn-based arterial implants. In vitro investigations that allow for a more realistic simulation of tissue or cell to material interactions could be beneficial both in clarifying complex biological response mechanisms and evaluating new material modifications.

Moving towards a more realistic testing framework in vivo may be more challenging. A major hurdle when investigating the in vivo reaction towards materials is the prevalence for evaluating materials in a healthy arterial environment. Large animal atherosclerotic models have been developed, but are expensive and generally not used as a direct human analog due to inconsistent disease presentation and lack of availability [155]. While producing statistically significant data with high sample sizes in large animal disease models may prove more challenging, the biological reaction towards the material could be more representative of the variability and chronic inflammatory environment encountered in human stent recipients. Additionally, material biocorrosion behavior could be more realistic. The atherosclerotic microenvironment is a dynamic and challenging cellular milieu. It contains an abundance of lipids in oxidized and non-oxidized forms, large amounts of inflammatory infiltrates with altered respiration patterns, and in most cases necrotic cores with a variety of leached intracellular contents [156, 157]. The inert metals of BMS often fail to prevent restenosis under these conditions. Taken together, the diseased human artery represents a more chemically aggressive environment for material oxidation to take place, and biocorrosion and its ensuing biological response could be dramatically different than in normal arteries with steady state microenvironments.

Over the past several decades, molecular biologists have successfully simulated human disease through genetic manipulation of small animals. Transgenic mice are now commonly used by cardiovascular researchers to study disease progression and therapies in pathogenic environments. Specifically, atherosclerotic mouse models are available that nominally replicate atherogenesis and spontaneous lesion development (eg. Apoe<sup>-/-</sup>, VLDL<sup>-/-</sup>). It should be straightforward to adapt the wire implantation model for use in mice (as transgenic variants are largely limited to mouse strains) to study the degradation profile and biologic response to biodegradable implants. Such an approach could represent a more realistic in vivo environment for evaluating the corrosion behavior of materials and the biological response to biodegradable metals.

## 6.2 Development of BRS manufacturing techniques

Lastly, alloy and process development for each bulk material to improve properties is continuously ongoing. There has been a push within the past five years to explore additive manufacturing techniques for biodegradable metals. This new processing strategy is still in its infancy, but could allow for corrosion rate control and use of patient specific dimensions. While additive manufacturing for Mg, Fe and Zn remain challenging for a variety of reasons [158], the benefits could be exceptional. The use of SLM has been demonstrated to produce reasonably small strut sizes for stent applications [159]. By means of appropriate design rules, stents with bifurcations and size variations in diameter and strut size can be achieved via the layer-by-layer manufacturing technique [160]. While several considerations remain largely unexplored such as the surface finish, the final mechanical strength, and the use of open-cell design [161], several recent studies show the use of biodegradable Zn [162] and Fe [163] alloys to produce stent mesh designs by SLM. On the other hand, the biological response to the AM produced struts is still underway with some initial works on the biological behavior reaching in-vivo stage for orthopedic use

[164], however the authors did not find studies that reported in vivo behavior of AM materials within the cardiovascular system.

### 6.3 Novel candidate metallic BRS materials

Recently, molybdenum was investigated in vitro to be used as a new biodegradable metal bulk material [165]. The authors reported uniform degradation in multiple solutions, with a corrosion rate that is optimal for use as cardiovascular stents. Pure molybdenum also has inherently good mechanical properties for a cardiovascular scaffold, which could limit its need for further manipulation and processing. While promising, the biocompatibility of this new bulk material remains to be evaluated, as molybdenum exists in trace concentrations within the body, possibly hinting at its lower toxicity threshold when compared to Mg, Fe, and Zn bulk materials.

## 7. Conclusions

Due to the complications associated with the permanent presence of stents, as well as the rising number of cardiovascular stents implanted in the clinic annually, BRSs have gained a lot of excitement over the past decade. BRSs aim to mitigate chronic stent thrombosis, restenosis, and inflammation by serving as a mechanical scaffold long enough for the host artery to remodel and heal before completely absorbing. While polymer BRSs exhibited suboptimal performance in clinical trials due to their deficient mechanical properties, metallic BRSs with improved mechanical strength have made their way into the clinic and have demonstrated more promising results. Mg based BRSs have passed clinical trials and received market approval in Europe. Although their success in the clinic marks a major step in the advancement of the BRS field, their mechanical strength and fast corrosion rate limits their application to shorter, more calcific lesions. As a result, developing Mg based BRS materials with improved mechanical strength and/or slower degradation rates remains a consistent pursuit. This has also created an opportunity for other metallic BRS materials. Fe BRS materials boast great mechanical strength and are currently involved in a clinical trial. However, the major limitation of Fe based BRSs is a slow degradation rate. The Fe based BRS sector remains active in its attempt to develop materials with increased corrosion rates, as well as improving our understanding of the biological response to the corrosion of these materials. Zn has emerged as a candidate BRS material due to its ideal corrosion rate and excellent biocompatibility but is limited by its mechanical strength. Active work in the Zn based BRS sector aims to develop new materials with improved mechanical strength, without sacrificing the excellent biocompatibility and corrosion rate exhibited by pure Zn. For all metallic BRS materials, the effects of surface treatments, alloying, and processing/manufacturing techniques on the resulting corrosion characteristics and ultimately the biological response should be investigated in detail. This will provide critical insight into developing novel BRS materials with corrosion characteristics that are finely tuned to optimize the biological response, leading to improved clinical outcomes.

## 7. Funding

This work was funded in part by Michigan Technological University

## 8. References

- [1] S.S. Virani, A. Alonso, E.J. Benjamin, M.S. Bittencourt, C.W. Callaway, A.P. Carson, A.M. Chamberlain, A.R. Chang, S. Cheng, F.N. Delling, Heart disease and stroke statistics—2020 update: a report from the American Heart Association, *Circulation* (2020) E139-E596.
- [2] E.J. Benjamin, S.S. Virani, C.W. Callaway, A.M. Chamberlain, A.R. Chang, S. Cheng, S.E. Chiuve, M. Cushman, F.N. Delling, R. Deo, Heart disease and stroke statistics—2018 update: a report from the American Heart Association, *Circulation* (2018).
- [3] B.E. Claessen, J.P. Henriques, F.A. Jaffer, R. Mehran, J.J. Piek, G.D.J.J.C.I. Dangas, Stent thrombosis: a clinical perspective, *7(10)* (2014) 1081-1092.
- [4] P.H. Grewe, T. Deneke, A. Machraoui, J. Barmeyer, K.-M.J.J.o.t.A.C.o.C. Müller, Acute and chronic tissue response to coronary stent implantation: pathologic findings in human specimen, *35(1)* (2000) 157-163.
- [5] T. Hu, J. Yang, K. Cui, Q. Rao, T. Yin, L. Tan, Y. Zhang, Z. Li, G. Wang, Controlled slow-release drug-eluting stents for the prevention of coronary restenosis: recent progress and future prospects, *ACS Applied Materials Interfaces* *7(22)* (2015) 11695-11712.
- [6] H. Jinnouchi, S. Torii, A. Sakamoto, F.D. Kolodgie, R. Virmani, A.V. Finn, Fully bioresorbable vascular scaffolds: lessons learned and future directions, *Nature Reviews Cardiology* *16(5)* (2019) 286-304.
- [7] S.-J. Park, S.-J. Kang, R. Virmani, M. Nakano, Y. Ueda, In-stent neoatherosclerosis: a final common pathway of late stent failure, *Journal of the American College of Cardiology* *59(23)* (2012) 2051-2057.
- [8] K. Yamaji, K. Inoue, T. Nakahashi, M. Noguchi, T. Domei, M. Hyodo, Y. Soga, S. Shirai, K. Ando, K. Kondo, Bare metal stent thrombosis and in-stent neoatherosclerosis, *Circulation: Cardiovascular Interventions* *5(1)* (2012) 47-54.
- [9] F. Otsuka, R.A. Byrne, K. Yahagi, H. Mori, E. Ladich, D.R. Fowler, R. Kutys, E. Xhepa, A. Kastrati, R. Virmani, Neoatherosclerosis: overview of histopathologic findings and implications for intravascular imaging assessment, *European heart journal* *36(32)* (2015) 2147-2159.
- [10] Y. Sotomi, Y. Onuma, C. Collet, E. Tenekecioglu, R. Virmani, N.S. Kleiman, P.W. Serruys, Bioresorbable scaffold: the emerging reality and future directions, *Circulation Research* *120(8)* (2017) 1341-1352.
- [11] J. Fu, Y. Su, Y.-X. Qin, Y. Zheng, Y. Wang, D. Zhu, Evolution of metallic cardiovascular stent materials: A comparative study among stainless steel, magnesium and zinc, *Biomaterials* *230* (2020) 119641.
- [12] Y. Zheng, X. Gu, F. Witte, Biodegradable metals, *Materials Science and Engineering: R: Reports* *77* (2014) 1-34.
- [13] S.H. Im, Y. Jung, S.H. Kim, Current status and future direction of biodegradable metallic and polymeric vascular scaffolds for next-generation stents, *Acta biomaterialia* *60* (2017) 3-22.
- [14] D.T.W. Yee, J.N.C. Koon, Y. Huang, P.W.E. Hou, H.L. Leo, S.S. Venkatraman, H.Y. Ang, Bioresorbable metals in cardiovascular stents: material insights and progress, *Materialia* (2020) 100727.
- [15] E. Mostaed, M. Sikora-Jasinska, J.W. Drelich, M. Vedani, Zinc-based alloys for degradable vascular stent applications, *Acta biomaterialia* *71* (2018) 1-23.
- [16] E. Mostaed, M. Sikora-Jasinska, M.S. Ardakani, A. Mostaed, I.M. Reaney, J. Goldman, J.W. Drelich, Towards revealing key factors in mechanical instability of bioabsorbable Zn-based alloys for intended vascular stenting, *Acta Biomaterialia* (2020).
- [17] C. Li, C. Guo, V. Fitzpatrick, A. Ibrahim, M.J. Zwierstra, P. Hanna, A. Lechtig, A. Nazarian, S.J. Lin, D.L. Kaplan, Design of biodegradable, implantable devices towards clinical translation, *Nature Reviews Materials* (2019) 1-21.

- [18] H.-S. Han, S. Loffredo, I. Jun, J. Edwards, Y.-C. Kim, H.-K. Seok, F. Witte, D. Mantovani, S. Glyn-Jones, Current status and outlook on the clinical translation of biodegradable metals, *Materials Today* 23 (2019) 57-71.
- [19] J.D. Abbott, C. Bavishi, Next-generation bioresorbable vascular scaffolds: When to get our hopes up?, *JACC: Cardiovascular Interventions*, 2019.
- [20] C. Rogers, S. Parikh, P. Seifert, E.R. Edelman, Endogenous cell seeding: remnant endothelium after stenting enhances vascular repair, *Circulation* 94(11) (1996) 2909-2914.
- [21] R.S. Schwartz, K.C. Huber, J.G. Murphy, W.D. Edwards, A.R. Camrud, R.E. Vlietstra, D.R. Holmes, Restenosis and the proportional neointimal response to coronary artery injury: results in a porcine model, *Journal of the American College of Cardiology* 19(2) (1992) 267-274.
- [22] J. Gunn, N. Arnold, K. Chan, L. Shepherd, D. Cumberland, D. Crossman, Coronary artery stretch versus deep injury in the development of in-stent neointima, *Heart* 88(4) (2002) 401-405.
- [23] A. Cornelissen, F.J. Vogt, The effects of stenting on coronary endothelium from a molecular biological view: Time for improvement?, *Journal of cellular and molecular medicine* 23(1) (2019) 39-46.
- [24] A. Kastrati, J. Mehilli, J. Dirschinger, F. Dotzer, H. Schühlen, F.-J. Neumann, M. Fleckenstein, C. Pfafferott, M. Seyfarth, A. Schömig, Intracoronary stenting and angiographic results: strut thickness effect on restenosis outcome (ISAR-STereo) trial, *Circulation* 103(23) (2001) 2816-2821.
- [25] C. Rogers, E.R. Edelman, Endovascular stent design dictates experimental restenosis and thrombosis, *Circulation* 91(12) (1995) 2995-3001.
- [26] J.M. Jiménez, P.F. Davies, Hemodynamically driven stent strut design, *Annals of biomedical engineering* 37(8) (2009) 1483-1494.
- [27] I. Moussa, C. Di Mario, B. Reimers, T. Akiyama, J. Tobis, A. Colombo, Subacute stent thrombosis in the era of intravascular ultrasound-guided coronary stenting without anticoagulation: frequency, predictors and clinical outcome, *Journal of the American College of Cardiology* 29(1) (1997) 6-12.
- [28] R. Kornowski, M.K. Hong, F.O. Tio, O. Bramwell, H. Wu, M.B. Leon, In-stent restenosis: contributions of inflammatory responses and arterial injury to neointimal hyperplasia, *Journal of the American College of Cardiology* 31(1) (1998) 224-230.
- [29] F.G. Welt, C.J.A. Rogers, thrombosis,, v. biology, *Inflammation and restenosis in the stent era*, 22(11) (2002) 1769-1776.
- [30] P. Libby, *Inflammation in atherosclerosis, Arteriosclerosis, thrombosis, and vascular biology* 32(9) (2012) 2045-2051.
- [31] J.H. Ip, V. Fuster, L. Badimon, J. Badimon, M.B. Taubman, J.H. Chesebro, Syndromes of accelerated atherosclerosis: role of vascular injury and smooth muscle cell proliferation, *Journal of the American College of Cardiology* 15(7) (1990) 1667-1687.
- [32] G.N. Levine, E.R. Bates, J.A. Bittl, R.G. Brindis, S.D. Fihn, L.A. Fleisher, C.B. Granger, R.A. Lange, M.J. Mack, L. Mauri, 2016 ACC/AHA guideline focused update on duration of dual antiplatelet therapy in patients with coronary artery disease: a report of the American College of Cardiology/American Heart Association Task Force on Clinical Practice Guidelines: an update of the 2011 ACCF/AHA/SCAI guideline for percutaneous coronary intervention, 2011 ACCF/AHA guideline for coronary artery bypass graft surgery, 2012 ACC/AHA/ACP/AATS/PCNA/SCAI/STS guideline for the diagnosis and management of patients with stable ischemic heart disease, 2013 ACCF/AHA guideline for the management of ST-elevation myocardial infarction, 2014 AHA/ACC guideline for the management of patients with non-ST-elevation acute coronary syndromes, and 2014 ACC/AHA guideline on perioperative cardiovascular evaluation and management of patients undergoing noncardiac surgery, *Circulation* 134(10) (2016) e123-e155.
- [33] W.C. Members, G.N. Levine, E.R. Bates, J.C. Blankenship, S.R. Bailey, J.A. Bittl, B. Cercek, C.E. Chambers, S.G. Ellis, R.A. Guyton, 2011 ACCF/AHA/SCAI guideline for percutaneous coronary intervention: a report of the American College of Cardiology Foundation/American Heart Association

- Task Force on Practice Guidelines and the Society for Cardiovascular Angiography and Interventions, *Circulation* 124(23) (2011) e574-e651.
- [34] P. Zartner, M. Buettner, H. Singer, M. Sigler, First biodegradable metal stent in a child with congenital heart disease: evaluation of macro and histopathology, *Catheterization and Cardiovascular Interventions* 69(3) (2007) 443-446.
- [35] P. Zartner, R. Cesnjevar, H. Singer, M. Weyand, First successful implantation of a biodegradable metal stent into the left pulmonary artery of a preterm baby, *Catheterization and Cardiovascular Interventions* 66(4) (2005) 590-594.
- [36] D. Schranz, P. Zartner, I. Michel-Behnke, H. Akintürk, Bioabsorbable metal stents for percutaneous treatment of critical recoarctation of the aorta in a newborn, *Catheterization and Cardiovascular Interventions* 67(5) (2006) 671-673.
- [37] C.J. McMahon, P. Oslizlok, K.P. Walsh, Early restenosis following biodegradable stent implantation in an aortopulmonary collateral of a patient with pulmonary atresia and hypoplastic pulmonary arteries, *Catheterization and Cardiovascular Interventions* 69(5) (2007) 735-738.
- [38] P. Peeters, M. Bosiers, J. Verbist, K. Deloose, B. Heublein, Preliminary results after application of absorbable metal stents in patients with critical limb ischemia, *Journal of Endovascular Therapy* 12(1) (2005) 1-5.
- [39] M. Bosiers, K. Deloose, J. Verbist, P. Peeters, First clinical application of absorbable metal stents in the treatment of critical limb ischemia: 12-month results, *Vasc Dis Manag* 2(4) (2005) 86-91.
- [40] M. Bosiers, A.I. Investigators, AMS INSIGHT—absorbable metal stent implantation for treatment of below-the-knee critical limb ischemia: 6-month analysis, *Cardiovascular and interventional radiology* 32(3) (2009) 424-435.
- [41] Y.H. Bouchi, B.D. Gogas, Biocorrosible metals for coronary revascularization: Lessons from PROGRESS-AMS, BIOSOLVE-I, and BIOSOLVE-II, *Global Cardiology Science and Practice* 2015(5) (2016) 63.
- [42] D.E. Cutlip, S. Windecker, R. Mehran, A. Boam, D.J. Cohen, G.-A. van Es, P. Gabriel Steg, M.-a.l. Morel, L. Mauri, P. Vranckx, Clinical end points in coronary stent trials: a case for standardized definitions, *Circulation* 115(17) (2007) 2344-2351.
- [43] R. Erbel, C. Di Mario, J. Bartunek, J. Bonnier, B. de Bruyne, F.R. Eberli, P. Erne, M. Haude, B. Heublein, M. Horrigan, Temporary scaffolding of coronary arteries with bioabsorbable magnesium stents: a prospective, non-randomised multicentre trial, *The Lancet* 369(9576) (2007) 1869-1875.
- [44] R. Waksman, R. Erbel, C. Di Mario, J. Bartunek, B. de Bruyne, F.R. Eberli, P. Erne, M. Haude, M. Horrigan, C. Ilesley, Early-and long-term intravascular ultrasound and angiographic findings after bioabsorbable magnesium stent implantation in human coronary arteries, *JACC: Cardiovascular Interventions* 2(4) (2009) 312-320.
- [45] M. Haude, R. Erbel, P. Erne, S. Verheye, H. Degen, D. Böse, P. Vermeersch, I. Wijnbergen, N. Weissman, F. Prati, Safety and performance of the drug-eluting absorbable metal scaffold (DREAMS) in patients with de-novo coronary lesions: 12 month results of the prospective, multicentre, first-in-man BIOSOLVE-I trial, *The Lancet* 381(9869) (2013) 836-844.
- [46] M. Haude, R. Erbel, P. Erne, S. Verheye, H. Degen, P. Vermeersch, N. Weissman, F. Prati, N. Bruining, R. Waksman, Safety and performance of the DRUG-Eluting Absorbable Metal Scaffold (DREAMS) in patients with de novo coronary lesions: 3-year results of the prospective, multicentre, first-in-man BIOSOLVE-I trial, *J EuroIntervention* 12(2) (2016) e160-6.
- [47] M. Haude, H. Ince, A. Abizaid, R. Toelg, P.A. Lemos, C. von Birgelen, E.H. Christiansen, W. Wijns, F.-J. Neumann, C. Kaiser, Safety and performance of the second-generation drug-eluting absorbable metal scaffold in patients with de-novo coronary artery lesions (BIOSOLVE-II): 6 month results of a prospective, multicentre, non-randomised, first-in-man trial, *The Lancet* 387(10013) (2016) 31-39.

- [48] M. Haude, H. Ince, A. Abizaid, R. Toelg, P.A. Lemos, C. von Birgelen, E.H. Christiansen, W. Wijns, F.-J. Neumann, C. Kaiser, Sustained safety and performance of the second-generation drug-eluting absorbable metal scaffold in patients with de novo coronary lesions: 12-month clinical results and angiographic findings of the BIOSOLVE-II first-in-man trial, *European heart journal* 37(35) (2016) 2701-2709.
- [49] H.M. Garcia-Garcia, M. Haude, K. Kuku, A. Hideo-Kajita, H. Ince, A. Abizaid, R. Tölg, P.A. Lemos, C. von Birgelen, E.H.J.I.j.o.c. Christiansen, In vivo serial invasive imaging of the second-generation drug-eluting absorbable metal scaffold (Magmaris—DREAMS 2G) in de novo coronary lesions: insights from the BIOSOLVE-II first-in-man trial, 255 (2018) 22-28.
- [50] M. Haude, H. Ince, R. Tölg, P.A. Lemos, C. von Birgelen, E.H. Christiansen, W. Wijns, F.-J. Neumann, E. Eeckhout, H.M. Garcia-Garcia, Safety and performance of the second-generation drug-eluting absorbable metal scaffold (DREAMS 2G) in patients with de novo coronary lesions: three-year clinical results and angiographic findings of the BIOSOLVE-II first-in-man trial, *Eurointervention: Journal of Europcr in Collaboration with the Working Group on Interventional Cardiology of the European Society of Cardiology* 15(15) (2020) e1375-e1382.
- [51] M. Haude, H. Ince, S. Kische, A. Abizaid, R. Tölg, P. Alves Lemos, N.M. Van Mieghem, S. Verheye, C. von Birgelen, E.H. Christiansen, Safety and clinical performance of a drug eluting absorbable metal scaffold in the treatment of subjects with de novo lesions in native coronary arteries: Pooled 12-month outcomes of BIOSOLVE-II and BIOSOLVE-III, *Catheterization and cardiovascular interventions* 92(7) (2018) E502-E511.
- [52] M. Haude, H. Ince, S. Kische, A. Abizaid, R. Tölg, L.P. Alves, N. Van Mieghem, S. Verheye, C. Von Birgelen, E. Christiansen, Sustained safety and clinical performance of a drug-eluting absorbable metal scaffold up to 24 months: pooled outcomes of BIOSOLVE-II and BIOSOLVE-III, *EuroIntervention* 13(4) (2017) 432-439.
- [53] Q. De Hemptinne, F. Picard, R. Briki, A. Awada, P.-G. Silance, D. Dolatabadi, N. Debbas, P. Unger, Drug-Eluting Resorbable Magnesium Scaffold Implantation in ST-Segment Elevation Myocardial Infarction: A Pilot Study, *The Journal of invasive cardiology* 30(6) (2018) 202-206.
- [54] M. Sabaté, F. Alfonso, A. Cequier, S. Romani, P. Bordes, A. Serra, A. Iñiguez, P. Salinas, B. García del Blanco, J. Goicolea, Magnesium-based resorbable scaffold versus permanent metallic sirolimus-eluting stent in patients with ST-segment elevation myocardial infarction: the MAGSTEMI randomized clinical trial, *Circulation* 140(23) (2019) 1904-1916.
- [55] S. Verheye, A. Wlodarczak, P. Montorsi, J. Torzewski, J. Bennett, M. Haude, G. Starmer, T. Buck, M. Wiemer, A.A. Nuruddin, BIOSOLVE-IV-registry: Safety and performance of the Magmaris scaffold: 12-month outcomes of the first cohort of 1,075 patients, *Catheterization Cardiovascular Interventions* (2020).
- [56] D. Siablis, P. Kraniotis, D. Karnabatidis, G.C. Kagadis, K. Katsanos, J. Tsolakis, Sirolimus-eluting versus bare stents for bailout after suboptimal infrapopliteal angioplasty for critical limb ischemia: 6-month angiographic results from a nonrandomized prospective single-center study, *Journal of Endovascular Therapy* 12(6) (2005) 685-695.
- [57] D. Scheinert, M. Ulrich, S. Scheinert, J. Sax, S. Bräunlich, G. Biamino, Comparison of sirolimus-eluting vs. bare-metal stents for the treatment of infrapopliteal obstructions, *EuroIntervention: journal of EuroPCR in collaboration with the Working Group on Interventional Cardiology of the European Society of Cardiology* 2(2) (2006) 169-174.
- [58] G. Ghimire, J. Spiro, R. Kharbanda, M. Roughton, P. Barlis, M. Mason, C. Ilsley, C. Di Mario, R. Erbel, R. Waksman, Initial evidence for the return of coronary vasoreactivity following the absorption of bioabsorbable magnesium alloy coronary stents, *EuroIntervention* 4(4) (2009) 481-4.

- [59] M.-C. Morice, P.W. Serruys, J.E. Sousa, J. Fajadet, E. Ban Hayashi, M. Perin, A. Colombo, G. Schuler, P. Barragan, G. Guagliumi, A randomized comparison of a sirolimus-eluting stent with a standard stent for coronary revascularization, *New England Journal of Medicine* 346(23) (2002) 1773-1780.
- [60] H. Li, H. Zhong, K. Xu, K. Yang, J. Liu, B. Zhang, F. Zheng, Y. Xia, L. Tan, D. Hong, Enhanced efficacy of sirolimus-eluting bioabsorbable magnesium alloy stents in the prevention of restenosis, *Journal of Endovascular Therapy* 18(3) (2011) 407-415.
- [61] E. Wittchow, N. Adden, J. Riedmüller, C. Savard, R. Waksman, M. Braune, Bioresorbable drug-eluting magnesium-alloy scaffold: design and feasibility in a porcine coronary model, *EuroIntervention* 8(12) (2013) 1441-1450.
- [62] J.M. Lasala, D.A. Cox, D. Dobies, K. Baran, W.B. Bachinsky, E.W. Rogers, J.A. Breall, D.H. Lewis, A. Song, R.M. Starzyk, Drug-eluting stent thrombosis in routine clinical practice: two-year outcomes and predictors from the TAXUS ARRIVE registries, *Circulation: Cardiovascular Interventions* 2(4) (2009) 285-293.
- [63] Y.B. Juwana, S. Rasoul, J.P. Ottervanger, H. Suryapranata, Efficacy and safety of rapamycin as compared to paclitaxel-eluting stents: a meta-analysis, 2010.
- [64] S. Windecker, M. Haude, F.-J. Neumann, K. Stangl, B. Witzenbichler, T. Slagboom, M. Sabaté, J. Goicolea, P. Barragan, S. Cook, Comparison of a novel biodegradable polymer sirolimus-eluting stent with a durable polymer everolimus-eluting stent: results of the randomized BIOFLOW-II trial, *Circulation: Cardiovascular Interventions* 8(2) (2015) e001441.
- [65] Y. Ueki, L. Räber, T. Otsuka, H. Rai, S. Losdat, S. Windecker, H.M. Garcia-Garcia, U. Landmesser, J. Koolen, R. Byrne, Mechanism of drug-eluting absorbable metal scaffold restenosis: a serial optical coherence tomography study, *Circulation: Cardiovascular Interventions* 13(3) (2020) e008657.
- [66] A. Hideo-Kajita, H.M. Garcia-Garcia, P. Kolm, V. Azizi, Y. Ozaki, K. Dan, H. Ince, S. Kische, A. Abizaid, R. Töelg, Comparison of clinical outcomes between Magmaris and Orsiro drug eluting stent at 12 months: Pooled patient level analysis from BIOSOLVE II–III and BIOFLOW II trials, *International journal of cardiology* 300 (2020) 60-65.
- [67] J.J. Wykrzykowska, R.P. Kraak, S.H. Hofma, R.J. van der Schaaf, E.K. Arkenbout, A.J. IJsselmuiden, J. Elias, I.M. van Dongen, R.Y. Tijssen, K.T. Koch, Bioresorbable scaffolds versus metallic stents in routine PCI, *New England Journal of Medicine* 376(24) (2017) 2319-2328.
- [68] Y. Onuma, Y. Sotomi, H. Shiomi, Y. Ozaki, A. Namiki, S. Yasuda, T. Ueno, K. Ando, J. Furuya, K. Igarashi, Two-year clinical, angiographic, and serial optical coherence tomographic follow-up after implantation of an everolimuseluting bioresorbable scaffold and an everolimus-eluting metallic stent: Insights from the randomised ABSORB Japan trial, *EuroIntervention* 12(9) (2016) 1090-1101.
- [69] B. Chevalier, Y. Onuma, A.J. van Boven, J.J. Piek, M. Sabaté, S. Helqvist, A. Baumbach, P.C. Smits, R. Kumar, L. Wasungu, Randomised comparison of a bioresorbable everolimus-eluting scaffold with a metallic everolimus-eluting stent for ischaemic heart disease caused by de novo native coronary artery lesions: the 2-year clinical outcomes of the ABSORB II trial, *EuroIntervention: journal of EuroPCR in collaboration with the Working Group on Interventional Cardiology of the European Society of Cardiology* 12(9) (2016) 1102-1107.
- [70] D. Mukherjee, Device thrombosis with bioresorbable scaffolds, *Mass Medical Soc*, 2017.
- [71] M. Haude, H. Ince, S. Kische, R. Toelg, N.M. Van Mieghem, S. Verheye, C. von Birgelen, E.H. Christiansen, E. Barbato, H.M. Garcia-Garcia, Sustained safety and performance of the second-generation sirolimus-eluting absorbable metal scaffold: Pooled outcomes of the BIOSOLVE-II and-III trials at 3 years, *Cardiovascular Revascularization Medicine* 21(9) (2020) 1150-1154.
- [72] Y. Ozaki, H.M. Garcia-Garcia, E. Shlofmitz, A. Hideo-Kajita, R. Waksman, Second-generation drug-eluting resorbable magnesium scaffold: review of the clinical evidence, *Cardiovascular Revascularization Medicine* 21(1) (2020) 127-136.

- [73] J. Fajadet, M. Haude, M. Joner, J. Koolen, M. Lee, R. Tölg, R. Waksman, Magmaris preliminary recommendation upon commercial launch: a consensus from the expert panel on 14 April 2016, *EuroIntervention: journal of EuroPCR in collaboration with the Working Group on Interventional Cardiology of the European Society of Cardiology* 12(7) (2016) 828-833.
- [74] A. Hideo-Kajita, H.G. Garcia, V. Azizi, H. Ince, S. Kische, A. Abizaid, R. Töelg, P. Lemos, N. Van Mieghem, S. Verheye, Comparison of clinical outcomes between magmaris (DREAMS 2G) and orsiro drug eluting stents: pooled patient level analysis from biosolve II-III and bioflow II trials, *Journal of the American College of Cardiology* 71(11 Supplement) (2018) A1109.
- [75] M.N. Tovar Forero, L. van Zandvoort, K. Masdjedi, R. Diletti, J. Wilschut, P.P. de Jaegere, F. Zijlstra, N.M. Van Mieghem, J.J.C. Daemen, C. Interventions, Serial invasive imaging follow-up of the first clinical experience with the Magmaris magnesium bioresorbable scaffold, 95(2) (2020) 226-231.
- [76] M. García-Guimaraes, P. Antuña, J. Cuesta, F.J.C. Alfonso, C. Interventions, Early restenosis of resorbable magnesium scaffolds: optical coherence tomography findings, 93(1) (2019) 79-81.
- [77] T. Marynissen, K. McCutcheon, J.J.C. Bennett, C. Interventions, Early collapse causing stenosis in a resorbable magnesium scaffold, 92(2) (2018) 310-312.
- [78] E. Cerrato, U. Barbero, J.A. Gil Romero, G. Quadri, H. Mejia-Renteria, F. Tomassini, F. Ferrari, F. Varbella, N. Gonzalo, J. Escaned, Magmaris™ resorbable magnesium scaffold: state-of-art review, *Future cardiology* 15(04) (2019) 267-279.
- [79] A. Vinogradov, E. Vasilev, V.I. Kopylov, M. Linderov, A. Brilevesky, D. Merson, High performance fine-grained biodegradable Mg-Zn-Ca alloys processed by severe plastic deformation, *Metals* 9(2) (2019) 186.
- [80] E. Mostaed, M. Sikora-Jasinska, L. Wang, A. Mostaed, I.M. Reaney, J.W. Drelich, Tailoring the mechanical and degradation performance of Mg-2.0 Zn-0.5 Ca-0.4 Mn alloy through microstructure design, *JOM* (2020) 1-12.
- [81] K. Guo, M. Liu, J. Wang, Y. Sun, W. Li, S. Zhu, L. Wang, S. Guan, Microstructure and texture evolution of fine-grained Mg-Zn-Y-Nd alloy micro-tubes for biodegradable vascular stents processed by hot extrusion and rapid cooling, *Journal of Magnesium and Alloys* 8(3) (2020) 873-882.
- [82] W. Lu, R. Yue, H. Miao, J. Pei, H. Huang, G. Yuan, Enhanced plasticity of magnesium alloy micro-tubes for vascular stents by double extrusion with large plastic deformation, *Materials Letters* 245 (2019) 155-157.
- [83] F. Kiani, C. Wen, Y. Li, Prospects and strategies for magnesium alloys as biodegradable implants from crystalline to bulk metallic glasses and composites—A review, *Acta Biomaterialia* 103 (2020) 1-23.
- [84] M. Jafary-Zadeh, G. Praveen Kumar, P.S. Branicio, M. Seifi, J.J. Lewandowski, F. Cui, A critical review on metallic glasses as structural materials for cardiovascular stent applications, *Journal of functional biomaterials* 9(1) (2018) 19.
- [85] G. Catalano, A.G. Demir, V. Furlan, B. Previtali, Laser microcutting of sheet metal for prototyping expandable stent-like structures in permanent and biodegradable alloys, 2017 IEEE 3rd International Forum on Research and Technologies for Society and Industry (RTSI), IEEE, 2017, pp. 1-5.
- [86] Y. Qin, P. Wen, H. Guo, D. Xia, Y. Zheng, L. Jauer, R. Poprawe, M. Voshage, J.H. Schleifenbaum, Additive manufacturing of biodegradable metals: Current research status and future perspectives, *Acta Biomaterialia* 98 (2019) 3-22.
- [87] A.G. Demir, Single track deposition study of biodegradable Mg-rare earth alloy by micro laser metal wire deposition, *Materials Today: Proceedings* 7 (2019) 426-434.
- [88] L. Jauer, W. Meiners, S. Vervoort, C. Gayer, N.A. Zumdick, D. Zander, Selective laser melting of magnesium alloys, European congress and exhibition on powder metallurgy. European PM Conference Proceedings, The European Powder Metallurgy Association, 2016, pp. 1-6.

- [89] N.A. Zumdick, L. Jauer, L.C. Kersting, T.N. Kutz, J.H. Schleifenbaum, D. Zander, Additive manufactured WE43 magnesium: A comparative study of the microstructure and mechanical properties with those of powder extruded and as-cast WE43, *Materials Characterization* 147 (2019) 384-397.
- [90] M. Esmaily, J. Svensson, S. Fajardo, N. Birbilis, G. Frankel, S. Virtanen, R. Arrabal, S. Thomas, L. Johansson, Fundamentals and advances in magnesium alloy corrosion, *Progress in Materials Science* 89 (2017) 92-193.
- [91] M. Dambatta, S. Izman, B. Yahaya, J. Lim, D. Kurniawan, Mg-based bulk metallic glasses for biodegradable implant materials: A review on glass forming ability, mechanical properties, and biocompatibility, *Journal of Non-Crystalline Solids* 426 (2015) 110-115.
- [92] J. Nagic, L.M. McCormick, R. Francis, N. Nerlekar, C. Jaworski, N.E. West, A.J. Brown, Novel bioabsorbable polymer and polymer-free metallic drug-eluting stents, *Journal of cardiology* 71(5) (2018) 435-443.
- [93] M. Echeverry-Rendon, J.P. Allain, S.M. Robledo, F. Echeverria, M.C. Harmsen, Coatings for biodegradable magnesium-based supports for therapy of vascular disease: A general view, *Materials Science and Engineering: C* 102 (2019) 150-163.
- [94] W. Chen, T.C. Habraken, W.E. Hennink, R.J. Kok, Polymer-free drug-eluting stents: an overview of coating strategies and comparison with polymer-coated drug-eluting stents, *Bioconjugate chemistry* 26(7) (2015) 1277-1288.
- [95] S. McGinty, T.T. Vo, M. Meere, S. McKee, C. McCormick, Some design considerations for polymer-free drug-eluting stents: a mathematical approach, *Acta biomaterialia* 18 (2015) 213-225.
- [96] M.-H. Kang, K.-H. Cheon, K.-I. Jo, J.-H. Ahn, H.-E. Kim, H.-D. Jung, T.-S. Jang, An asymmetric surface coating strategy for improved corrosion resistance and vascular compatibility of magnesium alloy stents, *Materials & Design* 196 (2020) 109182.
- [97] M.F. Maitz, M.C.L. Martins, N. Grabow, C. Matschegewski, N. Huang, E.L. Chaikof, M.A. Barbosa, C. Werner, C. Sperling, The blood compatibility challenge. Part 4: Surface modification for hemocompatible materials: Passive and active approaches to guide blood-material interactions, *Acta biomaterialia* 94 (2019) 33-43.
- [98] K. Zhou, Y. Li, L. Zhang, L. Jin, F. Yuan, J. Tan, G. Yuan, J. Pei, Nano-micrometer surface roughness gradients reveal topographical influences on differentiating responses of vascular cells on biodegradable magnesium, *Bioactive Materials* 6(1) (2020) 262-272.
- [99] S. Pacelli, S. Basu, J. Whitlow, A. Chakravarti, F. Acosta, A. Varshney, S. Modaresi, C. Berklund, A. Paul, Strategies to develop endogenous stem cell-recruiting bioactive materials for tissue repair and regeneration, *Advanced drug delivery reviews* 120 (2017) 50-70.
- [100] M. Peuster, P. Wohlsein, M. Brüggemann, M. Ehlerding, K. Seidler, C. Fink, H. Brauer, A. Fischer, G.J.H. Hausdorf, A novel approach to temporary stenting: degradable cardiovascular stents produced from corrodible metal—results 6–18 months after implantation into New Zealand white rabbits, 86(5) (2001) 563-569.
- [101] M. Peuster, C. Hesse, T. Schloo, C. Fink, P. Beerbaum, C.J.B. von Schnakenburg, Long-term biocompatibility of a corrodible peripheral iron stent in the porcine descending aorta, 27(28) (2006) 4955-4962.
- [102] R. Waksman, R. Pakala, R. Baffour, R. Seabron, D. Hellinga, F.O.J.J.o.i.c. Tio, Short-term effects of biocorrodible iron stents in porcine coronary arteries, 21(1) (2008) 15-20.
- [103] W. Lin, L. Qin, H. Qi, D. Zhang, G. Zhang, R. Gao, H. Qiu, Y. Xia, P. Cao, X. Wang, Long-term in vivo corrosion behavior, biocompatibility and bioresorption mechanism of a bioresorbable nitrided iron scaffold, *Acta biomaterialia* 54 (2017) 454-468.
- [104] Q. Feng, D. Zhang, C. Xin, X. Liu, W. Lin, W. Zhang, S. Chen, K. Sun, Characterization and in vivo evaluation of a bio-corrodible nitrided iron stent, *Journal of Materials Science: Materials in Medicine* 24(3) (2013) 713-724.

- [105] D. Pierson, J. Edick, A. Tauscher, E. Pokorney, P. Bowen, J. Gelbaugh, J. Stinson, H. Getty, C.H. Lee, J. Drelich, A simplified in vivo approach for evaluating the bioabsorbable behavior of candidate stent materials, *Journal of Biomedical Materials Research Part B: Applied Biomaterials* 100(1) (2012) 58-67.
- [106] W. Chao, Q. Hong, X.-y. HU, Y.-m. Ruan, T. Yi, C. Yan, X.-l. XU, X. Liang, T. Yue, R.-l. Gao, Short-term safety and efficacy of the biodegradable iron stent in mini-swine coronary arteries, *Chinese medical journal* 126(24) (2013) 4752-4757.
- [107] W.-J. Lin, D.-Y. Zhang, G. Zhang, H.-T. Sun, H.-P. Qi, L.-P. Chen, Z.-Q. Liu, R.-L. Gao, W. Zheng, Design and characterization of a novel biocorrosible iron-based drug-eluting coronary scaffold, *Materials & Design* 91 (2016) 72-79.
- [108] J.-F. Zheng, H. Qiu, Y. Tian, X.-Y. Hu, T. Luo, C. Wu, Y. Tian, Y. Tang, L.-F. Song, L. Li, Preclinical evaluation of a novel sirolimus-eluting iron bioresorbable coronary scaffold in porcine coronary artery at 6 months, *JACC: Cardiovascular Interventions* 12(3) (2019) 245-255.
- [109] J. Shi, X. Miao, H. Fu, A. Jiang, Y. Liu, X. Shi, D. Zhang, Z. Wang, In vivo biological safety evaluation of an iron-based bioresorbable drug-eluting stent, *BioMetals* (2020) 1-12.
- [110] Y. Qi, X. Li, Y. He, D. Zhang, J. Ding, Mechanism of acceleration of iron corrosion by a polylactide coating, *ACS applied materials & interfaces* 11(1) (2018) 202-218.
- [111] Y. Qi, H. Qi, Y. He, W. Lin, P. Li, L. Qin, Y. Hu, L. Chen, Q. Liu, H. Sun, Strategy of metal-polymer composite stent to accelerate biodegradation of iron-based biomaterials, *ACS applied materials & interfaces* 10(1) (2018) 182-192.
- [112] X. Li, W. Zhang, W. Lin, H. Qiu, Y. Qi, X. Ma, H. Qi, Y. He, H. Zhang, J. Qian, Long-Term Efficacy of Biodegradable Metal-Polymer Composite Stents After the First and the Second Implantations into Porcine Coronary Arteries, *ACS Applied Materials & Interfaces* 12(13) (2020) 15703-15715.
- [113] E. Scarcello, D. Lison, Are Fe-Based Stenting Materials Biocompatible? A Critical Review of In Vitro and In Vivo Studies, *Journal of Functional Biomaterials* 11(1) (2020) 2.
- [114] E. Scarcello, A. Herpain, M. Tomatis, F. Turci, P. Jacques, D. Lison, Hydroxyl radicals and oxidative stress: the dark side of Fe corrosion, *Colloids and Surfaces B: Biointerfaces* 185 (2020) 110542.
- [115] E. Scarcello, I. Lobysheva, C. Bouzin, P. Jacques, D. Lison, C. Dessy, Endothelial dysfunction induced by hydroxyl radicals—the hidden face of biodegradable Fe-based materials for coronary stents, *Materials Science and Engineering: C* (2020) 110938.
- [116] M. Schinhammer, I. Gerber, A.C. Hänzi, P.J. Uggowitzer, On the cytocompatibility of biodegradable Fe-based alloys, *Materials Science and Engineering: C* 33(2) (2013) 782-789.
- [117] D. Bian, L. Qin, W. Lin, D. Shen, H. Qi, X. Shi, G. Zhang, H. Liu, H. Yang, J. Wang, Magnetic resonance (MR) safety and compatibility of a novel iron bioresorbable scaffold, *Bioactive Materials* 5(2) (2020) 260-274.
- [118] C. Hehrlein, B. Schorch, N. Kress, A. Arab, C. von Zur Mühlen, C. Bode, T. Epting, J. Haberstroh, L. Mey, H. Schwarzbach, Zn-alloy provides a novel platform for mechanically stable bioresorbable vascular stents, *PloS one* 14(1) (2019) e0209111.
- [119] C. Zhou, H.-F. Li, Y.-X. Yin, Z.-Z. Shi, T. Li, X.-Y. Feng, J.-W. Zhang, C.-X. Song, X.-S. Cui, K.-L. Xu, Long-term in vivo study of biodegradable Zn-Cu stent: A 2-year implantation evaluation in porcine coronary artery, *Acta biomaterialia* 97 (2019) 657-670.
- [120] S. Lin, X. Ran, X. Yan, W. Yan, Q. Wang, T. Yin, J.G. Zhou, T. Hu, G. Wang, Corrosion behavior and biocompatibility evaluation of a novel zinc-based alloy stent in rabbit carotid artery model, *Journal of Biomedical Materials Research Part B: Applied Biomaterials* 107(6) (2019) 1814-1823.
- [121] P.K. Bowen, J. Drelich, J. Goldman, Zinc exhibits ideal physiological corrosion behavior for bioabsorbable stents, *Advanced materials* 25(18) (2013) 2577-2582.
- [122] H. Yang, C. Wang, C. Liu, H. Chen, Y. Wu, J. Han, Z. Jia, W. Lin, D. Zhang, W. Li, Evolution of the degradation mechanism of pure zinc stent in the one-year study of rabbit abdominal aorta model, *Biomaterials* 145 (2017) 92-105.

- [123] P.K. Bowen, J. Drelich, J.J.A.m. Goldman, Zinc exhibits ideal physiological corrosion behavior for bioabsorbable stents, *25(18)* (2013) 2577-2582.
- [124] C. Hehrlein, B. Schorch, J. Haberstroh, C. Bode, L. Mey, H. Schwarzbach, R. Kinscherf, S. Meckel, S. Schiestel, A. Kovacs, Bioresorbable zinc stent with ultra-thin center struts attenuates stent jail in porcine femoral artery bifurcations, *Minimally Invasive Therapy & Allied Technologies* (2020) 1-8.
- [125] H. Yang, B. Jia, Z. Zhang, X. Qu, G. Li, W. Lin, D. Zhu, K. Dai, Y. Zheng, Alloying design of biodegradable zinc as promising bone implants for load-bearing applications, *Nature communications* *11(1)* (2020) 1-16.
- [126] P. Libby, G.K. Hansson, Inflammation and immunity in diseases of the arterial tree: players and layers, *Circulation research* *116(2)* (2015) 307-311.
- [127] R.J. Guillory, A.A. Oliver, E.K. Davis, E.J. Earley, J.W. Drelich, J.J.J. Goldman, Preclinical in vivo evaluation and screening of zinc-based degradable metals for endovascular stents, *71(4)* (2019) 1436-1446.
- [128] P.K. Bowen, A. Drelich, J. Drelich, J. Goldman, Rates of in vivo (arterial) and in vitro biocorrosion for pure magnesium, *Journal of Biomedical Materials Research Part A* *103(1)* (2015) 341-349.
- [129] P.K. Bowen, R.J. Guillory II, E.R. Shearier, J.-M. Seitz, J. Drelich, M. Bocks, F. Zhao, J. Goldman, Metallic zinc exhibits optimal biocompatibility for bioabsorbable endovascular stents, *Materials Science Engineering: C* *56* (2015) 467-472.
- [130] A. Oliver, R.J. Guillory II, K.L. Flom, L.M. Morath, T.M. Kolesar, E. Mostaed, M. Sikora-Jasinska, J.W. Drelich, J. Goldman, Analysis of vascular inflammation against bioresorbable Zn-Ag based alloys, *ACS Applied Bio Materials* (2020).
- [131] R.J. Guillory, M. Sikora-Jasinska, J.W. Drelich, J. Goldman, In vitro corrosion and in vivo response to zinc implants with electropolished and anodized surfaces, *ACS applied materials interfaces* *11(22)* (2019) 19884-19893.
- [132] H. Jin, S. Zhao, R. Guillory, P.K. Bowen, Z. Yin, A. Griebel, J. Schaffer, E.J. Earley, J. Goldman, J.W. Drelich, Novel high-strength, low-alloys Zn-Mg (< 0.1 wt% Mg) and their arterial biodegradation, *Materials Science Engineering: C* *84* (2018) 67-79.
- [133] S. Zhao, J.-M. Seitz, R. Eifler, H.J. Maier, R.J. Guillory II, E.J. Earley, A. Drelich, J. Goldman, J.W.J.M.S. Drelich, E. C, Zn-Li alloy after extrusion and drawing: structural, mechanical characterization, and biodegradation in abdominal aorta of rat, *76* (2017) 301-312.
- [134] R.J. Guillory, P.K. Bowen, S.P. Hopkins, E.R. Shearier, E.J. Earley, A.A. Gillette, E. Aghion, M. Bocks, J.W. Drelich, J.J.A.B.S. Goldman, Engineering, Corrosion characteristics dictate the long-term inflammatory profile of degradable zinc arterial implants, *2(12)* (2016) 2355-2364.
- [135] R.J. Guillory II, T.M. Kolesar, A. Oliver, J.A. Stuart, M. Bocks, J.W. Drelich, J. Goldman, Zn<sup>2+</sup>-dependent suppression of vascular smooth muscle intimal hyperplasia from biodegradable zinc implants, *Materials Science Engineering: C* (2020) 110826.
- [136] E. Mostaed, M. Sikora-Jasinska, M.S. Ardakani, A. Mostaed, I.M. Reaney, J. Goldman, J.W. Drelich, Towards revealing key factors in mechanical instability of bioabsorbable Zn-based alloys for intended vascular stenting, *Acta biomaterialia* *105* (2020) 319-335.
- [137] E. Mostaed, M. Sikora-Jasinska, A. Mostaed, S. Loffredo, A.G. Demir, B. Previtali, D. Mantovani, R. Beanland, M. Vedani, Novel Zn-based alloys for biodegradable stent applications: design, development and in vitro degradation, *Journal of the mechanical behavior of biomedical materials* *60* (2016) 581-602.
- [138] A. Gokhan Demir, B. Previtali, Comparative study of CW, nanosecond-and femtosecond-pulsed laser microcutting of AZ31 magnesium alloy stents [J], *Biointerphases* *9(2)* (2014) 029004.
- [139] A.G. Demir, B. Previtali, C.A. Biffi, Fibre laser cutting and chemical etching of AZ31 for manufacturing biodegradable stents, *Advances in Materials Science and Engineering* *2013* (2013).

- [140] G. Catalano, A.G. Demir, V. Furlan, B. Previtali, Prototyping of biodegradable flat stents in pure zinc by laser microcutting and chemical etching, *Journal of Micromechanics and Microengineering* 28(9) (2018) 095016.
- [141] A.J. Drelich, S. Zhao, R.J. Guillory II, J.W. Drelich, J. Goldman, Long-term surveillance of zinc implant in murine artery: Surprisingly steady biocorrosion rate, *Acta biomaterialia* 58 (2017) 539-549.
- [142] S. Zhao, J.-M. Seitz, R. Eifler, H.J. Maier, R.J. Guillory II, E.J. Earley, A. Drelich, J. Goldman, J.W. Drelich, Zn-Li alloy after extrusion and drawing: structural, mechanical characterization, and biodegradation in abdominal aorta of rat, *Materials Science and Engineering: C* 76 (2017) 301-312.
- [143] P.K. Bowen, J.M. Seitz, R.J. Guillory, J.P. Braykovich, S. Zhao, J. Goldman, J.W. Drelich, Evaluation of wrought Zn–Al alloys (1, 3, and 5 wt% Al) through mechanical and in vivo testing for stent applications, *Journal of Biomedical Materials Research Part B: Applied Biomaterials* 106(1) (2018) 245-258.
- [144] H. Jin, S. Zhao, R. Guillory, P.K. Bowen, Z. Yin, A. Griebel, J. Schaffer, E.J. Earley, J. Goldman, J.W. Drelich, Novel high-strength, low-alloys Zn-Mg (< 0.1 wt% Mg) and their arterial biodegradation, *Materials Science and Engineering: C* 84 (2018) 67-79.
- [145] A.A. Shomali, R.J. Guillory, D. Seguin, J. Goldman, J.W. Drelich, Effect of PLLA coating on corrosion and biocompatibility of zinc in vascular environment, *Surface Innovations* 5(4) (2017) 211-220.
- [146] A.J. Drelich, P.K. Bowen, L. LaLonde, J. Goldman, J.W. Drelich, Importance of oxide film in endovascular biodegradable zinc stents, *Surface Innovations* 4(3) (2016) 133-140.
- [147] S. Torii, H. Jinnouchi, A. Sakamoto, M. Kutyna, A. Cornelissen, S. Kuntz, L. Guo, H. Mori, E. Harari, K.H. Paek, Drug-eluting coronary stents: insights from preclinical and pathology studies, *Nature Reviews Cardiology* (2019) 1-15.
- [148] R.A. Byrne, G.W. Stone, J. Ormiston, A. Kastrati, Coronary balloon angioplasty, stents, and scaffolds, *The Lancet* 390(10096) (2017) 781-792.
- [149] R. Virmani, F.D. Kolodgie, A.P. Burke, A. Farb, S.M. Schwartz, Lessons from sudden coronary death: a comprehensive morphological classification scheme for atherosclerotic lesions, *Arteriosclerosis, thrombosis, and vascular biology* 20(5) (2000) 1262-1275.
- [150] X. Liu, H. Yang, Y. Liu, P. Xiong, H. Guo, H.-H. Huang, Y. Zheng, Comparative studies on degradation behavior of pure zinc in various simulated body fluids, *Jom* 71(4) (2019) 1414-1425.
- [151] S. Johnston, Z. Shi, J. Venezuela, C. Wen, M.S. Dargusch, A. Atrens, Investigating Mg biocorrosion in vitro: lessons learned and recommendations, *JOM* 71(4) (2019) 1406-1413.
- [152] R.-Q. Hou, N. Scharnagl, R. Willumeit-Römer, F. Feyerabend, Different effects of single protein vs. protein mixtures on magnesium degradation under cell culture conditions, *Acta biomaterialia* 98 (2019) 256-268.
- [153] R.-Q. Hou, N. Scharnagl, F. Feyerabend, R. Willumeit-Römer, Exploring the effects of organic molecules on the degradation of magnesium under cell culture conditions, *Corrosion Science* 132 (2018) 35-45.
- [154] R. Hou, R. Willumeit-Römer, V.M. Garamus, M. Frant, J. Koll, F. Feyerabend, Adsorption of Proteins on Degradable Magnesium—Which Factors are Relevant?, *ACS applied materials & interfaces* 10(49) (2018) 42175-42185.
- [155] D. Wang, X. Xu, M. Zhao, X. Wang, Accelerated Miniature Swine Models of Advanced Atherosclerosis: A Review Based on Morphology, *Cardiovascular Pathology* (2020) 107241.
- [156] N. Leitinger, I.G. Schulman, Phenotypic polarization of macrophages in atherosclerosis, *Arteriosclerosis, thrombosis, and vascular biology* 33(6) (2013) 1120-1126.
- [157] G.J. Koelwyn, E.M. Corr, E. Erbay, K.J. Moore, Regulation of macrophage immunometabolism in atherosclerosis, *Nature immunology* 19(6) (2018) 526-537.
- [158] D. Carluccio, A. Demir, M. Bermingham, M. Dargusch, Challenges and Opportunities in the Selective Laser Melting of Biodegradable Metals for Load-Bearing Bone Scaffold Applications, *Metallurgical and Materials Transactions A: Physical Metallurgy and Materials Science* (2020).

- [159] A.G. Demir, B. Previtali, Additive manufacturing of cardiovascular CoCr stents by selective laser melting, *Materials & Design* 119 (2017) 338-350.
- [160] V. Finazzi, A.G. Demir, C.A. Biffi, C. Chiastra, F. Migliavacca, L. Petrini, B. Previtali, Design rules for producing cardiovascular stents by selective laser melting: Geometrical constraints and opportunities, 2019 International Conference on Stents: Materials, Mechanics and Manufacturing, ICS3M 2019, Elsevier BV, 2019, pp. 16-23.
- [161] V. Finazzi, A.G. Demir, C.A. Biffi, F. Migliavacca, L. Petrini, B. Previtali, Design and functional testing of a novel balloon-expandable cardiovascular stent in CoCr alloy produced by selective laser melting, *Journal of Manufacturing Processes* 55 (2020) 161-173.
- [162] P. Wen, M. Voshage, L. Jauer, Y. Chen, Y. Qin, R. Poprawe, J.H. Schleifenbaum, Laser additive manufacturing of Zn metal parts for biodegradable applications: processing, formation quality and mechanical properties, *Materials & Design* 155 (2018) 36-45.
- [163] J. Hufenbach, J. Sander, F. Kochta, S. Pilz, A. Voss, U. Kühn, A. Gebert, Effect of Selective Laser Melting on Microstructure, Mechanical, and Corrosion Properties of Biodegradable FeMnCS for Implant Applications, *Advanced Engineering Materials* (2020) 2000182.
- [164] D. Carluccio, C. Xu, J. Venezuela, Y. Cao, D. Kent, M. Bermingham, A.G. Demir, B. Previtali, Q. Ye, M. Dargusch, Additively manufactured iron-manganese for biodegradable porous load-bearing bone scaffold applications, *Acta Biomaterialia* 103 (2020) 346-360.
- [165] C. Redlich, P. Quadbeck, M. Thieme, B. Kieback, Molybdenum—A biodegradable implant material for structural applications?, *Acta Biomaterialia* 104 (2020) 241-251.